SYNTHESIS, CHARACTERIZATION, CONFORMATIONAL STUDY AND ANTIOXIDANT ACTIVITY OF *N*-ACYLHYDRAZONE DERIVATIEVES

By

Charles Lee Kuok Sui

A Final Year Project report submitted to the Department of Chemical Science,

Faculty of Science,

Universiti Tunku Abdul Rahman,

Bachelor of Science (Honours) Chemistry

October 2025

FACULTY OF SCIENCE

UNIVERSITI TUNKU ABDUL RAHMAN

COPYRIGHT STATEMENT

This Final Year Project Report is submitted in partial fulfilment of the requirements for the degree of **BACHELOR SCIENCE OF (HONS) CHEMISTRY** at Universiti Tunku Abdul Rahman (UTAR). This **Final Year Project Report** represents the work of the author, except where due acknowledgement has been made in the text. No part of this **Final Year Project Report** may be reproduced, stored, or transmitted in any form or by any means, whether electronic, mechanical, photocopying, recording, or otherwise, without the prior written permission of the author or UTAR, in accordance with UTAR's Intellectual Property Policy.

ABSTRACT

SYNTHESIS, CHARACTERIZATION, CONFORMATIONAL STUDY AND ANTIOXIDANT ACTIVITY OF *N*-ACYLHYDRAZONE DERIVATIEVES

CHARLES LEE KUOK SUI

A series of *N*-acylhydrazone derivatives (**SB 1-SB 8**) were successfully synthesized in yields ranging from 68% to 97% through the condensation of a carboxylic acid hydrazide with various benzaldehydes bearing different substituents. The structures of the synthesized compounds were confirmed by FTIR, ^{1}H NMR, ^{13}C NMR, DEPT-135, NOE, HMQC, and HMBC spectral analyses.

Based on the relative configuration of the imine (C=N) double bond and the conformation of the amide [C(=O)–NH] bond, the C=N double bonds of the *N*-acylhydrazones were assigned the *E* configuration. Furthermore, the NMR data of all synthesized compounds indicated the presence of both *cis* and *trans* conformers. The population ratio of *cis* conformers ranged from 32% to 60%, while that of *trans* conformers ranged from 41% to 68%. The rotational barriers of the *cis*/*trans* conformers were determined to be between 73.47 and 77.81 kJ/mol.

The antioxidant activity of the synthesized *N*-acylhydrazone derivatives was evaluated using the DPPH assay. Apart from **SB 7**, which exhibited weak

antioxidant activity, the compounds did not demonstrate significant antioxidant properties.

Keywords: Benzaldehyde, Hydrazide, Hydrazone, Indole, NMR, DPPH, Antioxidant

Subject Area: QD241-441 Organic Chemistry

ABSTRAK

SINTESIS, KARAKTERISASI, KAJIAN KONFORMASI DAN AKTIVITI ANTIOKSIDAN DERIVATIF *N*-ASILHIDRAZON

CHARLES LEE KUOK SUI

Siri derivatif *N*-asilhidrazon (**SB 1–SB 8**) telah disintesis dengan hasil antara 68.22% hingga 96.64% melalui tindak balas pemeluwapan antara asid karboksilik hidrazida dengan pelbagai benzaldehid yang mempunyai berbeza substituen. Struktur sebatian yang disintesis telah disahkan melalui analisis spektrum FTIR, ^{1}H NMR, ^{13}C NMR, DEPT-135, NOEdiff, HMQC dan HMBC.

Berdasarkan konfigurasi relatif ikatan berganda imina (C=N) serta konformasi ikatan amida [C(=O)–NH], ikatan berganda C=N dalam *N*-asillhidrazon telah ditentukan mempunyai konfigurasi *E*. Selain itu, data NMR bagi semua sebatian yang disintesis menunjukkan kewujudan konformer cis dan trans. Nisbah populasi konformer *cis* adalah antara 31.97% hingga 59.52%, manakala konformer *trans* adalah antara 40.48% hingga 68.03%. Halangan putaran bagi konformer *cis/trans* ditentukan berada dalam julat 73.47 hingga 77.81 kJ/mol.

Aktiviti antioksida derivatif *N*-asillhidrazon yang disintesis telah dinilai menggunakan ujian DPPH. Selain **SB 7** yang menunjukkan aktiviti antioksida lemah, sebatian lain tidak memperlihatkan sifat antioksida yang signifikan.

ACKNOWLEDGEMENT

First and foremost, I would like to express my sincere gratitude to my supervisor, Dr. Sim Kooi Mow, for his invaluable guidance, continuous support, and constructive advice throughout the course of this project. It has been a great privilege to learn under Dr. Sim, whom I would regard as an expert in his field. I am also deeply thankful to the laboratory officer for the technical assistance, without which the completion of this project would not have been as smooth.

I would also like to extend my heartfelt appreciation to my friends for their emotional support during this journey. In particular, I am especially grateful to my senior, Yong Jing Yi, for the constant encouragement, motivation, and generous sharing of knowledge and experience, which have greatly helped me.

My deepest thanks also go to my family, for their unconditional love, patience, and understanding. Thank you for always being there to listen, to support me in times of difficulty, and for bearing with me during moments of stress and pressure.

Lastly, I thank God. Through Him, I can do all things.

DECLARATION

I hereby declare that this final year project report is based on my original work, except for quotations and citations which have been appropriately acknowledged. I also declare that this report has not been previously or concurrently submitted for any other degree at UTAR or any other institution.

(**CHARLES LEE KUOK SUI**)

APPROVAL SHEET

This final year project report entitled "**SYNTHESIS, CHARACTERIZATION, CONFORMATIONAL STUDY AND ANTIOXIDANT ACTIVITY OF *N*-ACYLHYDRAZONE DERIVATIEVES**" was completed by **CHARLES LEE KUOK SUI** and submitted as partial fulfilment of the requirements for the degree of Bachelor of Science (Honours) Chemistry at Universiti Tunku Abdul Rahman.

Approved by:

_____

Dr. Sim Kooi Mow Date:

Supervisor

Department of Chemical Science

Faculty of Science

Universiti Tunku Abdul Rahman

FACULTY OF SCIENCE

UNIVERSITI TUNKU ABDUL RAHMAN

Date:

PERMISSION SHEET

It is hereby certified that **CHARLES LEE KUOK SUI** (ID No: **22ADB04202**) has completed this final year project report entitled "**SYNTHESIS, CHARACTERIZATION, CONFORMATIONAL STUDY AND ANTIOXIDANT ACTIVITY OF *N*-ACYLHYDRAZONE DERIVATIEVES**" under the supervision of Associate Professor Dr. Sim Kooi Mow from the Department of Chemical Science, Faculty of Science.

I hereby give permission to the University to upload the softcopy of my final year project report in pdf format into the UTAR Institutional Repository, which may be made accessible to the UTAR community and public.

Yours truly,

(**CHARLES LEE KUOK SUI**)

TABLE OF CONTENTS

LIST OF TABLES

LIST OF FIGURES

LIST OF SCHEMES

LIST OF SYMBOLS AND ABBREVIATIONS

g/mol	Gram per mole
mmol	Millimole
μM	Micromolar
NAH	*N*-acylhydrazone
TLC	Thin Layer Chromatography
R_f	Retardation factor
DPPH	2,2-Diphenyl-1-picrylhydrazyl
IC_{50}	Half-maximal Inhibitory Concentration
FTIR	Fourier Transform Infrared Spectroscopy
nm	Wavelength
NMR	Nuclear Magnetic Resonance
DEPT	Distortionless Enhancement by Polarization Transfer
HMBC	Heteronuclear Multiple Quantum Correlation
HMQC	Heteronuclear Multiple Bond Correlation
NOE	Nuclear Overhauser Effect
Hz	Hertz
J	Coupling constant
s	Singlet
d	Doublet
dd	Doublet of doublets

td	Triplet of doublets
δ	Chemical shift
δ_H	Chemical shift of proton
δ_C	Chemical shift of carbon
T_c	Coalescence temperature
$\Delta\nu$	Peak separation
k_c	Rate constant of cis/trans equilibrium
$\Delta G^{\neq}$	Energy of rotational barrier
kJ/mol	Kilojoule per mole

CHAPTER 1

INTRODUCTION

1.1 Indole

Indole is classified as a heterocyclic aromatic compound, also named as benzopyrrole, due to its fused bicyclic structure consisting of a benzene ring and a pyrrole ring (Chauhan, Saxena and Saha, 2021). The molecular formula for indole is C_8H_7N and its molecular weight is 117.15 g/mol (PubChem, 2020). As an electron-rich species, it is basic in nature. It can be produced in the bacterial degradation of amino acid tryptophan. Naturally present in human faeces, it is identified by an intensive faecal odour. However, at low concentrations, it exhibits a pleasant flowery smell and is a composition of many flower scents and perfumes. Furthermore, indole moieties exist in many biological active compounds and neurotransmitter serotonin. Therefore, due to the crucial roles acted by indole and its derivatives in biological systems, there are intensively studied for their biological properties.

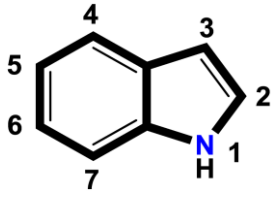

Figure 1. 1: Chemical structure of indole

1.1.1 Application of Indole

In the medicinal industry, indole is regarded as one of the most privileged scaffolds due to its remarkable ability to interact with various receptors, contributing rise to a wide range of biological activities (Barresi et al., 2024). As a result, indole derivatives have become a crucial class of compounds in medicinal chemistry, due to their wide-ranging biological activities and therapeutic potential (Mo et al., 2024). For instance, indomethacin, a nonsteroidal anti-inflammatory drug (NSAID) consisting of an indole moiety, has been commonly utilized in treatment of fever, pain, and inflammation. Thus, due to their attractive properties, the presence of indole nucleus in therapeutic agents, including but is not limited to anti-HIV, anti-inflammatory, antihypertensive, antileukemia and antimigraine.

1.1.1.1 Antioxidant Activity

The natural and synthetic indole derivatives, such as melatonin and serotonin and its derivatives, including 5-hydroxutryptofol, 5-methoxytryptamine, and 5-methoxytryptofol, have attracted great attention, due to their antioxidant activity that prevent the oxidative stress and reactive oxygen species (ROS)-induced cellular damage (Jasiewicz et al., 2021).

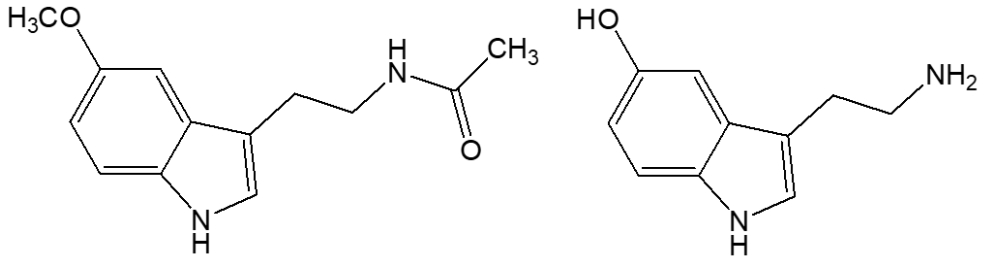

Figure 1. 2: Chemical structure of melatonin and serotonin

1.1.1.2 Anticancer Activity

Furthermore, according to Dhiman, Sharma and Singh (2022), trimethoxy phenyl linked indole derivatives act as tubulin polymerization inhibitors by blocking cellular mitosis. Tubulin polymerization inhibition prevents the proper formation of microtubules. Since microtubules are protein subunits in the long chains of tubulin and play a crucial role in cell division, they have become important targets in anticancer drug development. The indole moiety contributes to disrupting microtubules and dissolving mitotic spindles, thereby hindering tubulin polymerization.

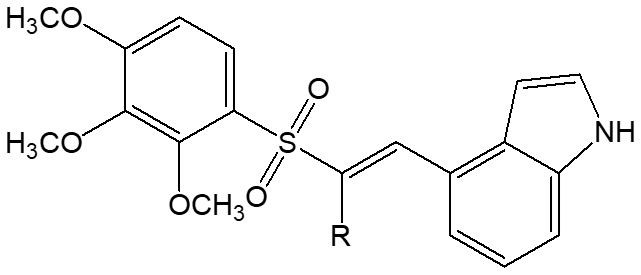

Figure 1. 3: General chemical structure of trimethoxy phenyl-based indole

1.1.1.3 Antimalarial Activity

In addition, the indole derivatives have demonstrated significant antimalarial activity. Malaria, which is a life-threatening disease, is caused by infection with *Plasmodium falciparum*. Based on the research by Luthra et al. (2019), luzindole which is an indole derivative, was discovered to disrupt the cell cycle of parasite and inhibit the growth of *P. falciparum* in low micromolar IC_{50} value.

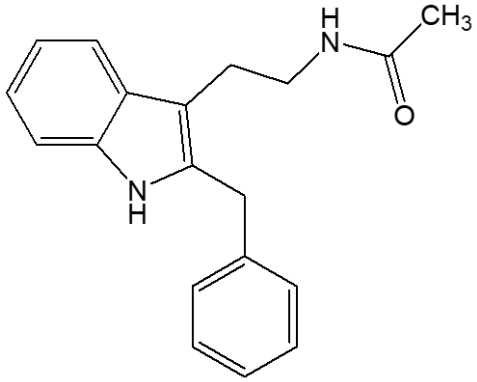

Figure 1. 4: Chemical structure of luzindole

1.2 Hydrazide

Hydrazides are the compounds consisting of the group -C(=O)-NH-N-, which is their functional group. In the functional group, the hydrazine moiety, -N-N-, is bonded to an acyl group (Moldoveanu, 2019). Hydrazides are formed by the replacement of a hydrogen from hydrazine with an acyl group. Typically, the hydrazides can be synthesized via the condensation of an ester or a carboxylic acid with hydrazine.

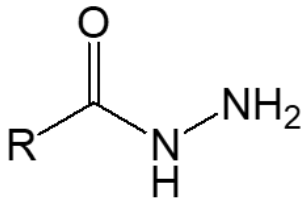

Figure 1. 5: General chemical structure of hydrazide

1.2.1 Application of Hydrazide

Hydrazides have shown a wide range of applications. The diverse chemical structures of hydrazides contribute to broad bioactivity (Le Goff and Ouazzani, 2014). Their biological activities arise from various mechanisms, including enzyme inhibition, metal ion chelation and interaction with biomolecules. Numerous scientific studies have reported their biological properties such as antibacterial, antifungal and anticancer activities (Łukasz Popiołek, 2023). In addition to their biological applications, hydrazides also serve as crucial intermediate in the synthesis of heterocyclic systems.

1.2.1.1 Anti-inflammatory Activity

Hydrazides have demonstrated anti-inflammatory potential, which is commonly attributed to their enzymes' inhibition ability. For instance, according to Panaskar, Jain and Mohanty (2022), the synthesized novel chalcone hydrazide derivatives

exhibited the anti-inflammatory activity in the carrageenan-induced paw oedema model in rat.

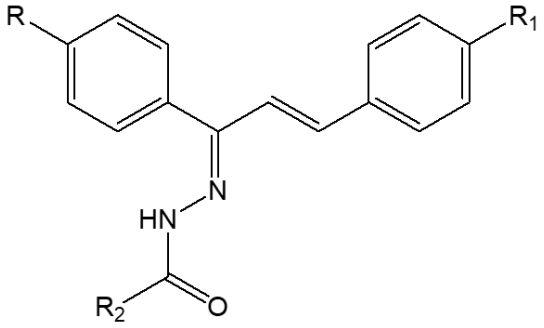

Figure 1. 6: General chemical structure of chalcone hydrazide derivatives

1.2.1.2 Antibacterial Activity

Furthermore, hydrazides will show diverse clinical properties according to the nature of attached substituents. Hydrazide-derived azetidine-2-ones exhibit notable antibacterial activity (Łukasz Popiołek, 2023). Based on the research (Sulthana and Quine, 2015), hydrazides serve as versatile starting materials that can undergo certain reaction to form azetidine-2-ones, which display the antibacterial activity against *Bacillus subtilis*, *Staphylococcus aureus*, *Escherichia coli*, and *Pseudomonas aeruginosa*.

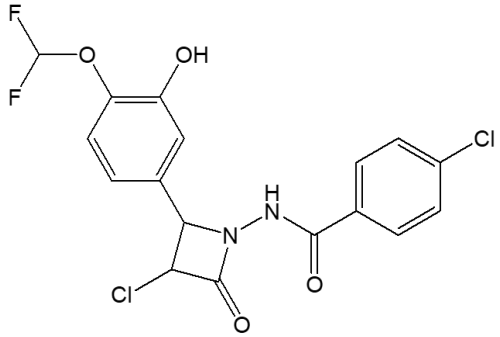

Figure 1. 7: Chemical structure of azeditin-2-one derivative

1.2.1.1 Antifungal Activity

Additionally, hydrazide-containing *L*-perillaldehyde derivatives have been revealed to display antifungal properties against plant pathogenic fungi. They act as the fungicides by inducing remarkable morphological alternations and accumulation of reactive oxygen species, leading to mycelial growth inhibition and oxidative damage in fungi (Gong et al., 2025).

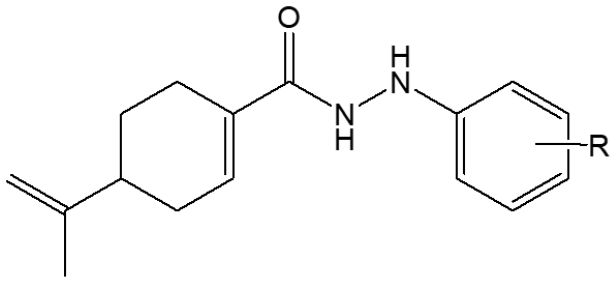

Figure 1. 8: General chemical structure of hydrazide-containing *L*-perillaldehydes

1.3 Hydrazone

Hydrazones, a class of organic compounds with the general structure shown in **Figure 1.9**, are formed through the condensation reaction between hydrazine and carbonyl compounds, such as ketones or aldehydes, in the presence of an acidic catalyst under alcoholic conditions (Lawrence et al., 2019). Among hydrazones, *N*-acylhydrazones, the targeted products of this project, represent a particularly important subclass and are characterized by the presence of an acyl group attached to the hydrazone moiety. The structural backbone of *N*-acylhydrazones, -C(=O)-

NH-N=CH-, contains an electrophilic carbon atom at the imine group (CH=N), a nucleophilic imine nitrogen bearing an electron lone pair (CH=N:), and an amino nitrogen with acidic properties (-NH-). Therefore, *N*-acylhydrazones exhibit both electrophilic and nucleophilic behaviour (Socea et al., 2022). The nucleophilic attack occurs at the amide nitrogen (-NH-), whereas electrophilic attack takes place at the carbonyl oxygen (C=O).

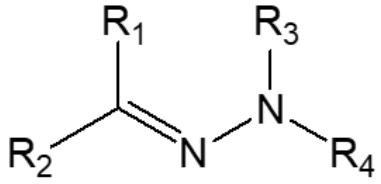

Figure 1. 9: General chemical structure of hydrazones

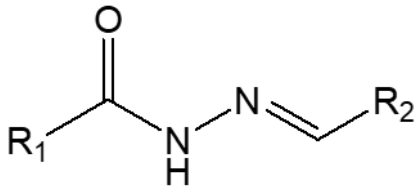

Figure 1. 10: General chemical structure of *N*-acylhydrazones

1.3.1 Application of *N*-acylhydrazone

N-acylhydrazones (NAHs) have demonstrated notable versatility, with promising applications in both drug design and medicinal chemistry. This adaptability is significantly attributed to the synthesis simplicity (Vlad et al., 2024). As a subclass of hydrazone, NAHs are synthesized through the condensation of hydrazides with carbonyl compounds, such as ketones and aldehydes. Based on their interactions with a wide range of biological targets, NAH fragments have been incorporated

into numerous bioactive compounds. Reported biological properties of NAHs include antibacterial, antimycobacterial, analgesic, and anti-inflammatory activities.

1.3.1.1 Antioxidant Activity

Among the various pharmacological properties of *N*-acylhydrazones, antioxidant property of NAHs, which is also one of the studies of my project, has been investigated. According to Simijonović et al. (2023), the synthesized coumarin *N*-acylhydrazone derivatives shown antioxidant potential with obtaining IC_{50} values ranging from 2.1 to 3.2 μM in the DPPH assay.

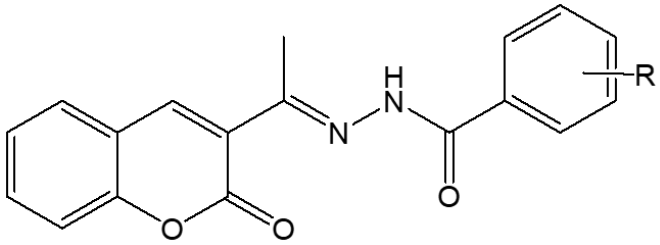

Figure 1. 11: General chemical structure of coumarin *N*-acylhydrazones

1.3.1.2 Antibacterial Activity

Several developed medicinal compounds containing NAH scaffolds, such as nitrofurantoin and nitrofurazone, are recognized as useful antibacterial agent. The activated nitrofurantoin and nitrofurazone act as antibacterial substance by

inhibiting bacterial enzymes which are responsible in DNA and RNA synthesis, carbohydrate metabolism and essential metabolic processes (Guay, 2001).

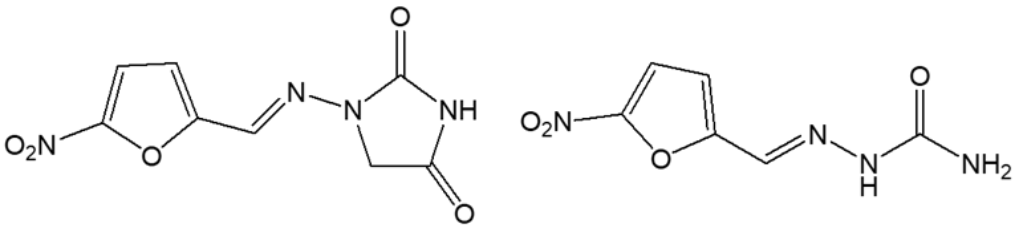

Figure 1. 12: Chemical structure of nitrofurantoin and nitrofurazone

1.3.1.3 Antifungal Activity

Furthermore, benzimidazole derivatives bearing an *N*-acyhydrazone moiety have also been demonstrated antifungal activity. According to the research by Özkay et al. (2010), such derivatives shown in **Figure 1.12** exhibit antifungal property against certain fungal strains.

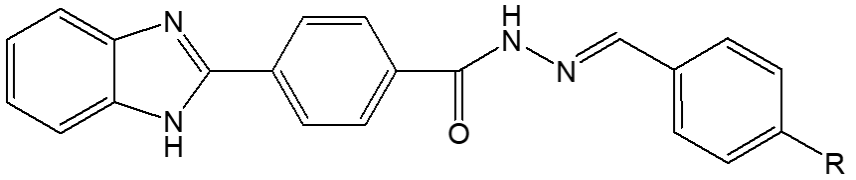

Figure 1. 13: General chemical structure of benzimidazole-hydrazones

1.3.2 Isomerism of *N*-acylhydrazone

As mentioned previously, the -C(=O)-NH-N=CH- moiety forms the backbone of *N*-acylhydrazones. This backbone formed through the combination of amide and imine functional groups, which enables the molecule to exhibit both geometric and conformational stereoisomerism. Geometric (*E/Z*) isomerism and conformational (*syn* and *anti*) isomerism result from restricted rotation around the imine bond (C=N) and the amide bond [C(=O)–NH], respectively.

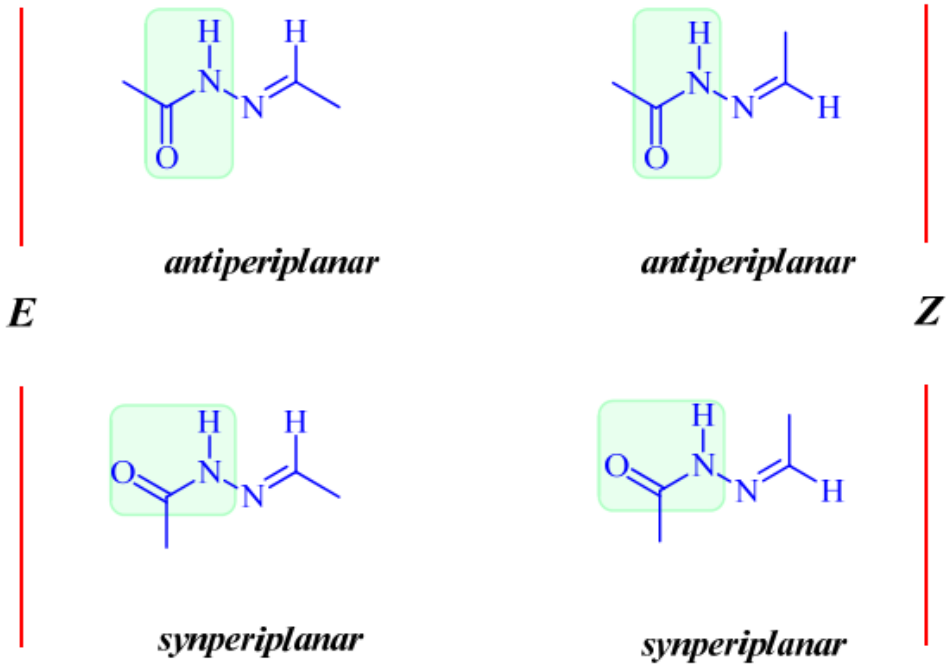

Figure 1. 14: Four possible isomers of *N*-acylhydrazones

Theoretically, four possible isomers of *N*-acylhydrazones are estimated to exist. However, the *E* isomer predominates over the *Z* isomer, due to its geometry with reduced steric hindrance (Munir et al., 2021). Among the *E* isomers, the *syn*

conformer exists at a higher abundancy than the *anti* conformer due to its greater stability (Kumar et al., 2017).

1.4 Antioxidant Activity

In molecular biology, degenerative processes are associated with an excess of free radicals, which promote oxidative reactions harmful to the body (Munteanu and Apetrei, 2021). Over the past three decades, oxidative stress is an attractive concept which is widely utilized in medical science, as it acts as a key role in the development of numerous diseases, including diabetes, hypertension, acute renal failure, Alzheimer's, and Parkinson's. During cellular oxygen metabolism, reactive oxygen species (ROS) are generated, which can initiate oxidation by transferring oxygen to other molecules. Some ROS exist as free radicals containing unpaired electrons, making them exhibit the common properties of radical, like highly unstable and reactive (Lobo et al., 2010). Therefore, antioxidants play a crucial to mitigate oxidative stress.

Antioxidants are substances that prevent intracellular oxidation molecules (Rao, 2016), typically by donating electrons or hydrogen atoms. As mentioned above, free radicals formed during oxygen metabolism are reactive and can initiate chain reactions that leads to cellular damage or even cell death. According to the illustration shown in **Figure 1.15**, antioxidants neutralize free radicals by donating

an electron, thereby terminating the chain reaction. Through this way, antioxidants function as reducing agents.

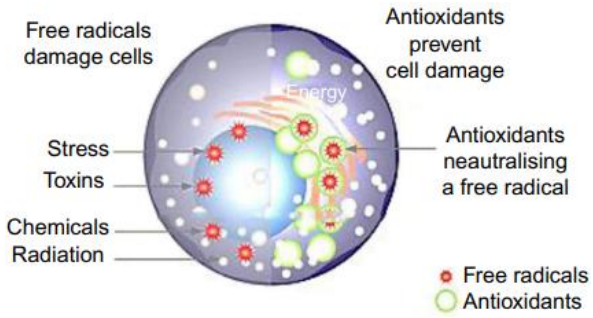

Figure 1. 15: Cellular oxidation reaction

1.4.1 Determination of Half-Maximal Inhibitory Concentration (IC_{50})

Half-maximal inhibitory concentration (IC_{50}) is a widely utilized parameter for evaluating drug efficacy. It represents the concentration of a compound required to suppress a biological process by 50% (Aykul and Martinez-Hackert, 2016). In antioxidant activity assessment, the IC_{50} value indicates to the concentration of an antioxidant needed to scavenge 50% of free radicals in a specific assay, such as the DPPH assay.

To determine the IC_{50} value, a series of sample solution with different concentrations is prepared and subjected to a free radical assay. The percentage of free radical scavenging activity at each concentration is then measured. Based on the collected data, a dose-response curve can be obtained. The concentration of the sample that achieves 50% inhibition is interpolated and defined as the IC_{50} value.

Therefore, a lower IC_{50} value indicates stronger capability in free radical scavenging, and hence, greater antioxidant activity.

1.5 Objectives of Research

1. To synthesize a series of *N*-acylhydrazones.
2. To characterize the structure of *N*-acylhydrazones via NMR, FTIR, and melting point.
3. To determine the relative configuration of the imine double bond and amide group of *N*-acylhydrazones by using NOE experiments.
4. To determine the rotational barriers around the N-C(=O) bond for *N*-acylhydrazones by using Dynamic NMR experiments.
5. To evaluate the antioxidant activity of *N*-acylhydrazones by using the DPPH assay.

CHAPTER 2

LITERATURE REVIEW

2.1 Synthesis of Indole

The presence of indole ring system is widely observed in biologically active medicinal agents and natural products. Among the various method of indole synthesis, the Fischer indole reaction, which was discovered in 1883 by Emil Fischer, remain the most extensively utilized in the indole synthesis (Humphrey and Kuethe, 2006). In this approach, a phenylhydrazone is initially formed through the condensation of an enolizable carbonyl compound, ketone or aldehyde compounds, with phenylhydrazine. Under acidic conditions and elevated temperature, the phenylhydrazone undergoes tautomerization to anamine, which then proceeds through a [3,3]-sigmatrophic shift to generate diimine intermediate. This is followed by rearomatization, intramolecular cyclization and the elimination of ammonia to yield the desired indole (Simoneau and Ganem, 2008).

Scheme 2. 1: Fischer indole reaction

Since the process have been invented more than a century, the applicable catalysts of reaction have broadened to include various Lewis acids, Bronsted acids and acidic solid supports.

In a paper by Li et al. (2019), substituted indole compounds were yielded through the conventional method, Fischer indole reaction, using phenylhydrazine hydrochloride and ethyl levulinate as starting materials. In their procedure, equimolar amounts of the reagents were added to acetic acid with sodium acetate. The mixture was heated for 5-10 minutes at 70 °C. After the removal of solvent, the residue was followed by the reflux process for 3-4 hours in ethanol with concentrated sulphuric acid added as the catalyst.

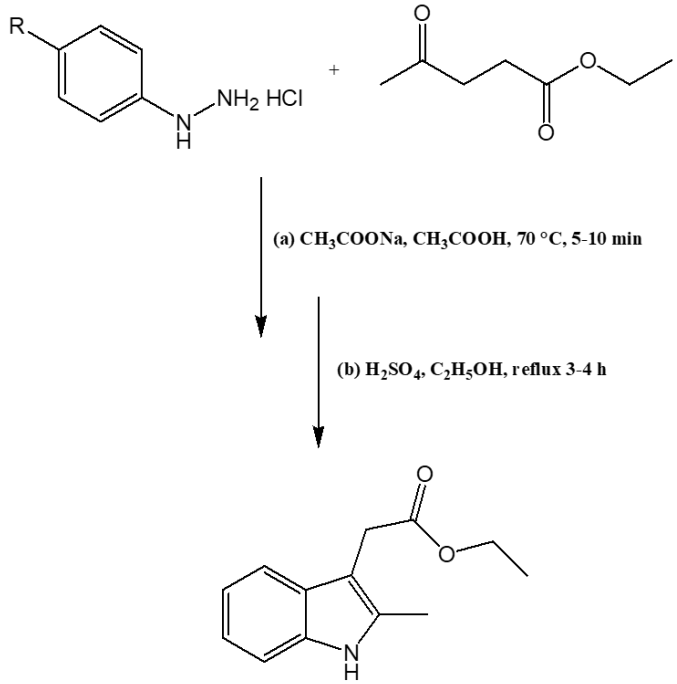

Scheme 2. 2: Fischer indole synthesis pathway (Li et al., 2019)

Apart from the conventional method, a greener approach to Fischer indole synthesis has been demonstrated through the application of conductively heated sealed-vessel reactor. In a study by Cirillo, Caccavale, and DeLuna (2021), indole was

synthesized using 1.00 mmol of phenyl hydrazine hydrochloride salt and 1.00 mmol of dehydroepiandrosterone (DHEA) acetate as reactants. A suspension was prepared in 2 mL of glacial acetic acid, then placed in the heating cavity of the reactor and heated at 160 °C for 20 minutes. The reaction yielded products with a percentage yield ranging from 40% to 60%.

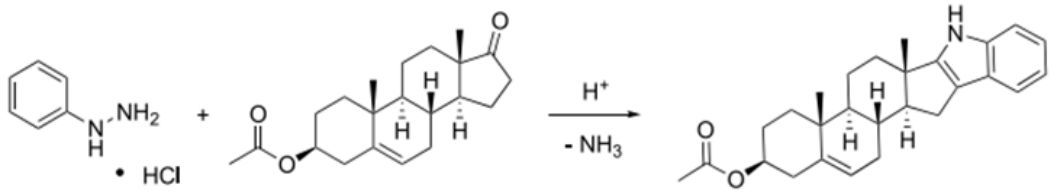

Scheme 2. 3: Fisher indole synthesis using phenyl hydrazine and dehydroepiandrostenone (DHEA) acetate

2.2 Synthesis of Carboxylic Acid Hydrazide

Carboxylic acid hydrazides are the valuable intermediate in the organic synthesis due to their high versatility. It can be synthesized though several methods, however in the general approach, carboxylic acid hydrazide can be synthesized through the hydrazinolysis of esters. Besides that, the carbodiimide coupling of carboxylic acids with hydrazides is the less common method (Hermanson, 2013). In the method, the carboxylate will be activated to form an intermediate that then reacts with the hydrazide nucleophile.

In the synthesis demonstrated by Zhang et al. (2018), they successfully obtained carboxylic acid hydrazide by reacting previously prepared indole ester with

hydrazine hydrate under reflux ethanol. An upstanding percentage of yield, which is 90%, was achieved in their synthetic pathway.

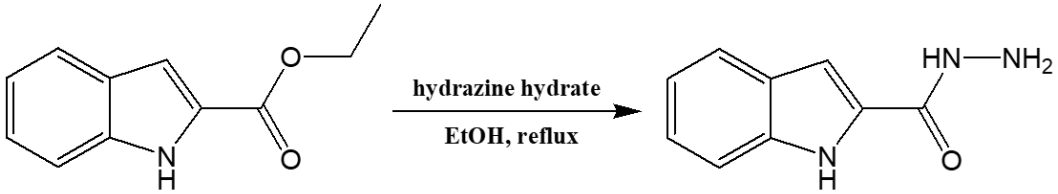

Scheme 2. 4: Synthesis of carboxylic acid hydrazide (Zhang et al., 2018)

Apart from conventional method, in the synthesis demonstrated by Aboul-Fadl et al. (2011), they employed green chemistry tools by utilizing microwave irradiation in the synthesis of fenamic hydrazides. In the microwave-assisted method, fenamic hydrazides were directly obtained from the reaction of acids with hydrazine hydrate. The products were achieved in excellent yield (82%-96%) under microwave irradiation with condition at 300 W and 250 °C for 4-12 minutes. In comparison, the conventional heating method required the use of solvent, sulphuric acid as a catalyst, and two synthetic steps, consuming 15-28 hours to produce an overall yield ranging from 64-86%. Therefore, the microwave-assisted synthetic pathway displayed superior efficiency in terms of time, yield and sustainability.

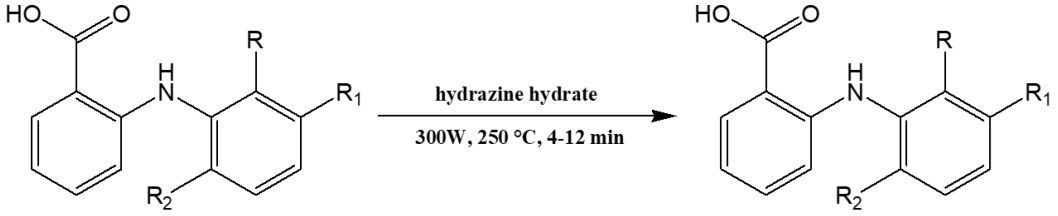

Scheme 2. 5: Microwave-assisted one-step synthesis of fenamic hydrazides

Furthermore, a study by Halloran, Hudecek, and Burkart (2023) demonstrated a continuous-flow process as an alternative approach for the large-scale production. As the illustration shown in **Scheme 2.6**, the hydrazinolysis of carboxylic acids

under flow conditions obtained acid hydrazides in high yields ranging from 81% to 91%. The method employed short residence times, around 13 to 25 minutes and showed excellent substrate tolerance.

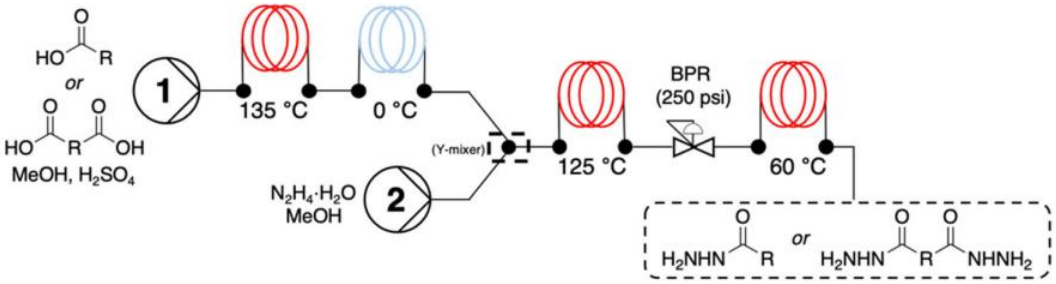

Scheme 2. 6: Telescoped flow process for the synthesis of Acid Hydrazides

2.3 Synthesis of *N*-acylhydrazones

Initiating from the corresponding carboxylic acid hydrazide, *N*-acylhydrazones can be prepared through the condensation reaction between the hydrazide and the carbonyl compound. Based on this general principle of the reaction, there are various approaches to synthesize *N*-acylhydrazones.

According to the study by Vlad et al. (2024), (*EZ*)-N'-benzylidene-2-(6-chloro-9*H*-carbazol-2-yl)propanehydrazide derivatives can be synthesized with microwave-assisted condition. In their synthesis, 0.001 mol of 2-(6-chloro-9*H*-carbazol-2-yl)propanehydrazide and 0.001 mol of different aromatic aldehydes were placed into a microwave tube, followed by the addition of 3 mL of absolute methanol and 4 drops of glacial acetyl acid as the catalyst. The reaction mixture was pre-stirred for 5 minutes and then subjected to microwave irradiation at 90 °C for 25 minutes

under strong absorption. Upon the completion of reaction, the mixture was cooled to room temperature and subsequently stored in a refrigerator overnight. The obtaining product was filtered and recrystallized from a 1:2 mixture of isopropanol and water.

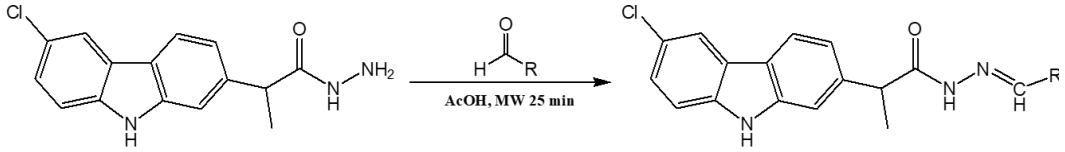

Scheme 2. 7: Synthetic pathway for the (*EZ*)-N'-benzylidene-2-(6-chloro-9*H*-carbazol-2-yl)propanehydrazide derivatives

Munir et al. (2021) published another method which is similar to Vlad et al., but without the assistance of microwave irradiation. In their work, 5 mmol of 2-(6-methyl-1*H*-pyrazolo[3,4-*b*]quinolin-1-yl)acetohydrazide was condensed with 5 mmol of different aromatic aldehydes under reflux in ethanol with addition of catalytic amount of orthophosphoric acid. The precipitated products were collected by filtration, washed with cold ethanol, dried in an oven, and recrystallized from absolute ethanol. Excellent yields were achieved, ranging from 82 to 99%.

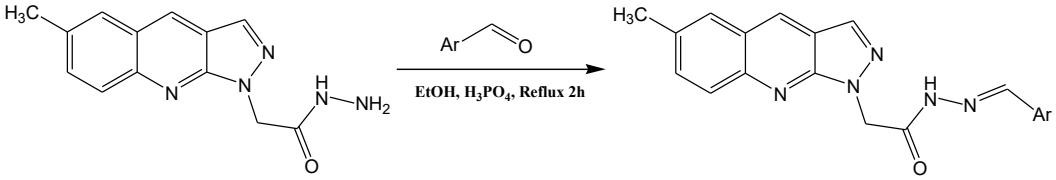

Scheme 2. 8: Synthesis of *N*-acylhydrazone derivatives from 2-(6-methyl-1*H*-pyrazolo[3,4-*b*]quinolin-1-yl)acetohydrazide

Gu et al. (2012) reported another method that adopting the similar methodological approach as Munir et al. (2021). A series of *N*-acylhydrazone derivatives was synthesized, performing good yields of 65-92%. In their procedure, 2 mmol of dehydroabietic acid hydrazide was dissolved in 20 mL of absolute ethanol, followed

by addition of an equimolar amount of substituted aromatic aldehyde and 2 drops of glacial acetic acid. The mixture was refluxed for 2-3 hours, the progress of the reaction monitored by TLC. After completing the reaction, the mixture was poured into cold water and allowed to stand for 4 hours. The resulting precipitate was also collected by filtration, washed with water and recrystallized from ethanol to obtain desired *N*-acylhydrazone derivatives.

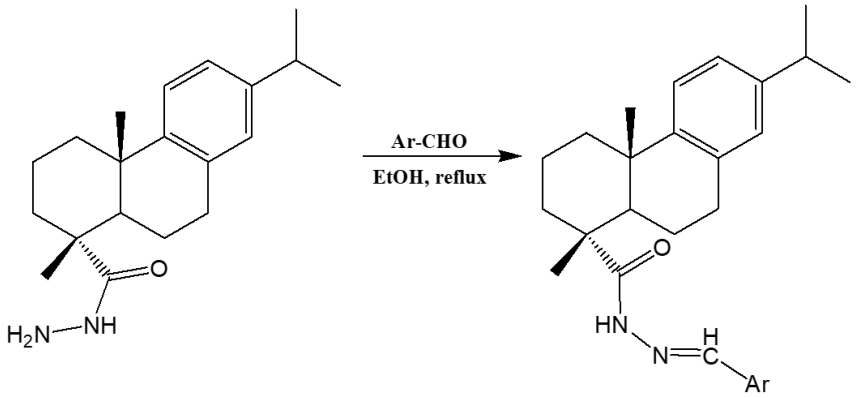

Scheme 2. 9: Synthesis of *N*-acylhyrazone derivatives from dehydroabietic acid hydrazide

2.4 Conformational Study of *N*-acylhydrazones

Due to the presence of –C(=O)-NH-N=C- moiety, *N*-acylhydrazones exhibit the isomerism. To investigate their conformational behaviour, NMR spectroscopy is a widely employed method. NMR is well established as a tool for structural elucidation of compounds; it is also a reliable method in the study of spatial arrangement and kinetic of the compounds.

2.4.1 NMR Spectra of *N*-acylhydrazones

In the synthesis of the analgesic lead compound LASSBio-1083 by Lopes et al. (2013), they reported the duplication of proton signals in the ^{1}H-NMR spectrum. This duplication was assumed as the attribution of the presence of two geometric isomers (*E/Z*) arising from the imine (C=N) bond.

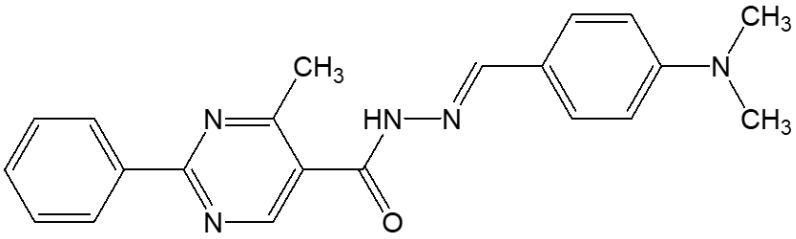

Figure 2. 1: Chemical structure of compound LASSBio-1083

Here's the ^{1}H-NMR spectra of compound LASSBio-1083 obtained by Lopes et al.:

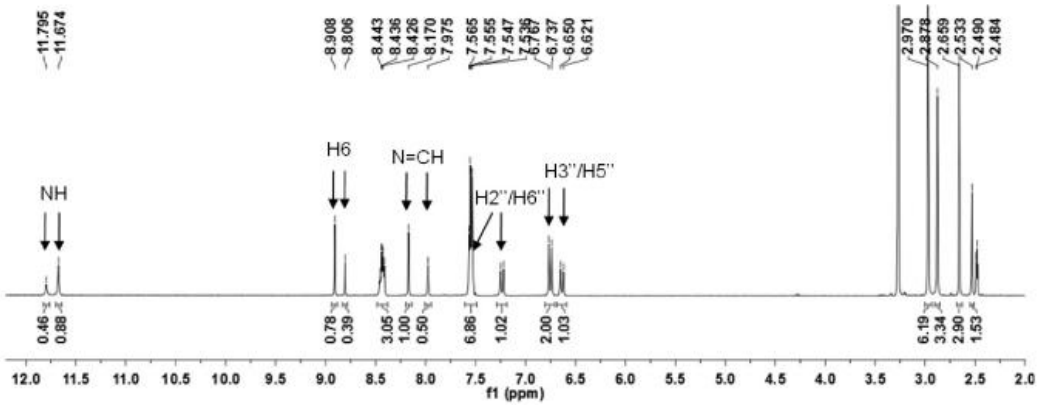

Figure 2. 2: ^{1}H-NMR spectra of compound LASSBio-1083

According to the study by Hamzi, Barhoumi-Slimi and Abidi (2016), two NH signals of the -C(=O)-NH-N=C- moiety were observed. In the *trans* isomer, the NH signal appeared further downfield compared to the *cis* isomer, which helps in assigning the corresponding peaks to each isomer. Moreover, by comparing the

integrals of the same proton signal for each isomer, the ratio of each isomer can be determined.

2.4.2 Determination of the Relative Configuration of *N*-acylhydrazones

Lopes et al. (2013) proceed the study of relative configuration of compound LASSBio-1083 with differential Nuclear Overhauser Effect (NOEdiff) experiments. The amide proton (NH) was selected for irradiation. Based on their finding, due to spatial angle and distance factors, only E isomers were observed, the Z isomer were not detected.

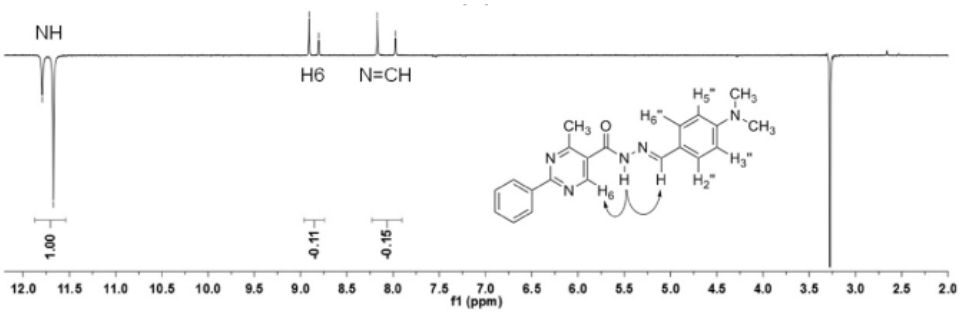

Figure 2. 3: NOEdiff spectra for irradiation of NH of compound LASSBio-1083

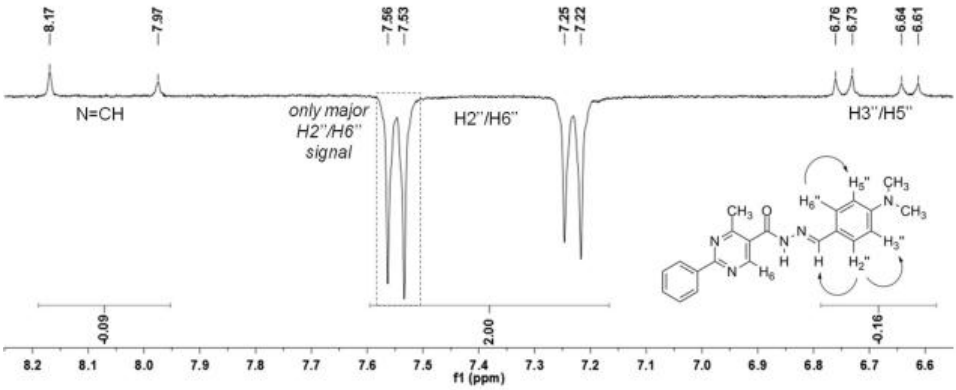

Figure 2. 4: Expanded NOEdiff spectra for irradiation of (H_2''/H_6'') of compound LASSBio-1083

2.4.3 Dynamic Studies of the CO-NH Rotational Barrier

Due to the presence of an N-N single bond in *N*-acylhydrazones that makes rotation is possible, leading to the interchange between conformers. As result, there are two conformational isomers of *N*-acylhydrazones exist in equilibrium, which causes in the appearance of two peaks in the NMR spectra. By applying dynamic NMR, the rotational barrier between these two isomers can be determined. Determination of coalescence temperature is one of the approaches in conducting dynamic NMR experiments.

According to the study by Hamzi, Barhoumi-Slimi and Abidi (2016), the merging of *cis* and *trans* signals was observed with gradually increasing temperature. When the signals of *cis* and *trans* isomers coalesce into single peak, the corresponding temperature was identified as the coalescence temperature (T_c). Through T_c, the rate constant (k_c) can be calculated using the equation [$k_c = (\pi/\nu)/2^{1/2}$]. Hence, from the value of rate constant, the Gibbs free energy of activation ($\Delta G^{\neq}$) can be obtained using Eyring equation: $\Delta G^{\neq} = 19.14T_c\,(10.32 + \log T_c/k_c) \times 10^{-3}$ with unit kJ/mol.

Figure 2.5 and **Figure 2.6** show one of the *N*-acylhydrazones synthesized by Hamzi, Barhoumi-Slimi and Abidi and the ^{1}H NMR spectrum at various temperatures.

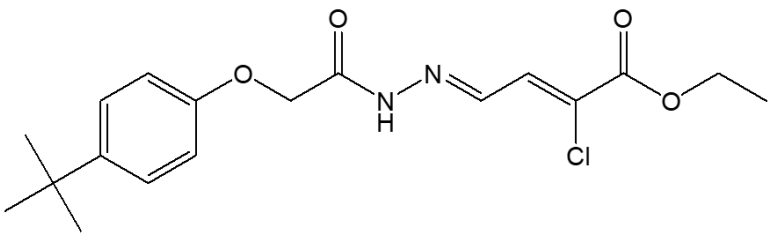

Figure 2. 5: Chemical structure of a synthesized *N*-acylhydrazone by Hamzi, Barhoumi-Slimi and Abidi

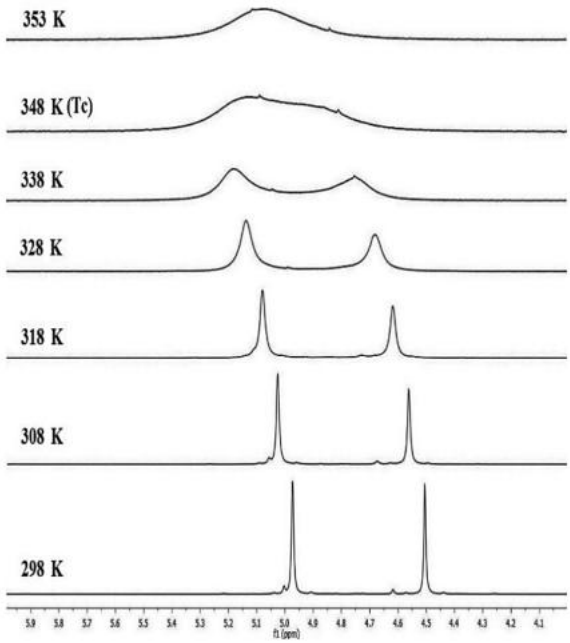

Figure 2. 6: ^{1}H NMR spectra of the -OCH_2 signals of the **Figure 2.5** *N*-acylhydrazone at variable temperatures

2.5 Antioxidant Activity Evaluation of *N*-acylhydrazones

In the measurement of antioxidant activity, there are a variety of methods can be used, including DPPH, hydroxyl radical scavenging assay and O^{2-} scavenging capacity assay (Liang and Kitts, 2014). Among the methods, the DPPH assay is the

widely utilized method due to its conveniency and efficiency. 1,1-Diphenyl-2-picryl-hydrazyl (DPPH) is a stable radical that consists of an unpaired electron at one atom of the nitrogen bridge (Sharma and Bhat, 2009). The presence of odd electrons displays an intensive absorption band at a wavelength of 517 nm, as the absorption band will be weakened once the odd electron is paired off by a hydrogen from the antioxidant.

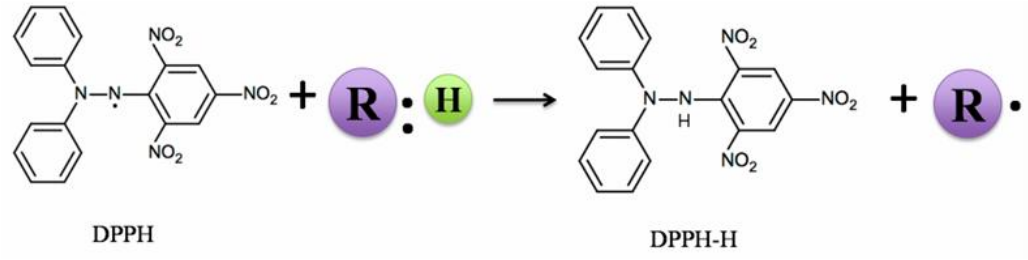

Figure 2. 7: Reaction mechanism of DPPH with antioxidant

Therefore, DPPH, which is purple in colour, will be converted to yellow colour, and the percentage of radical scavenging can be determined by measuring the absorbance of the mixture of DPPH and antioxidants at 517 nm.

According to the study by Boubekri et al. (2024), the antioxidant activity of a series of *N*-acylhydrazones was evaluated using the DPPH assay. Solution of the compounds was prepared in dimethyl sulfoxide (DMSO) at a concentration of 100 µg/mL. Increasing volumes of these solutions were sampled and diluted with methanol to a final volume for 0.2 mL. Each prepared sample solution was then mixed with a 2.4 µg/mL of methanolic DPPH solution. The mixtures were then stirred and incubate in dark at ambient temperature for 30 minutes. After incubation, the absorbance was measured at 517 nm, using methanol as the blank and ascorbic

acid as control. Each measurement was performed triplicate and the IC_{50} values of the *N*-acylhydrazones were subsequently calculated.

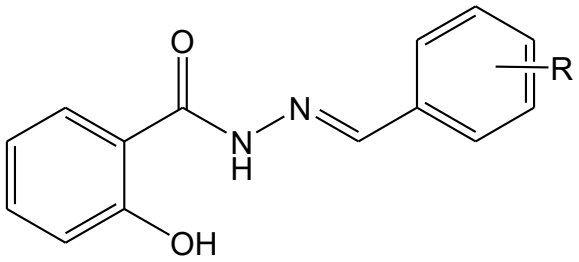

Figure 2. 8: General chemical structure of *N*-acylhydrazones by Boubekri et al.

CHAPTER 3

MATERIALS AND METHODOLOGY

3.1 Chemical Used

Table 3. 1: Chemicals used for the synthesis of carboxylic acid hydrazide

Chemical Name **Molecular Formula**	**Molecular Weight** **$gmol^{-1}$**	**Manufacturer** **Country**	**State**
Acetic Acid CH_3COOH	60.05	Merck, Germany	Liquid
Absolute Ethanol C_2H_5OH	46.07	Fisher Scientific, UK	Liquid
Concentrated Hydrochloric Acid HCl	36.46	Fisher Scientific, UK	Liquid
Hydrazine Hydrate $NH_2NH_2 \cdot H_2O$	50.06	Synerlab, France	Liquid
Anhydrous Sodium Sulphate Na_2SO_4	142.04	Merck, Germany	Solid

Table 3. 2: Chemical used in the extraction of carboxylic acid hydrazide

Chemical Name **Molecular Formula**	**Molecular Weight** **$gmol^{-1}$**	**Manufacturer** **Country**	**State**
Ethyl Acetate $CH_3COOC_2H_5$	88.11	RCI Labscan, Thailand	Liquid

Table 3. 3: Chemicals used in the synthesis of *N*-acylhydrazones

Chemical Name **Molecular Formula**	**Molecular Weight** **$gmol^{-1}$**	**Manufacturer** **Country**	**State**
4-Methylbenzaldehyde C_8H_8O	120.15	Merck, Germany	Liquid
2-Chlorobenzaldehyde C_7H_5ClO	140.57	Merck, Germany	Liquid
4-Chlorobenzaldehyde C_7H_5ClO	140.57	Merck, Germany	Solid
2,4-Dichlorobenzaldehyde $C_7H_4Cl_2O$	175.01	Merck, Germany	Solid
3,4-Dichlorobenzaldehyde $C_7H_4Cl_2O$	175.01	Merck, Germany	Solid
2-hydroxybenzaldehyde $C_7H_6O_2$	122.12	Merck, Germany	Liquid
4-hydroxybenzaldehyde $C_7H_6O_2$	122.12	Merck, Germany	Solid
4-Nitrobenzaldehyde $C_7H_5NO_3$	151.12	Merck, Germany	Solid
Absolute Ethanol C_2H_5OH	46.07	Fisher Scientific, UK	Liquid

Table 3. 4: Chemicals used in recrystallization of *N*-acylhydrazones

Chemical Name **Molecular Formula**	**Molecular Weight** **$gmol^{-1}$**	**Manufacturer** **Country**	**State**
95% Ethanol C_2H_5OH	46.07	Chemical Industries (Malaya), Malaysia	Liquid

Table 3. 5: Chemicals used in TLC analysis

Chemical Name **Molecular Formula**	**Molecular Weight** **$gmol^{-1}$**	**Manufacturer** **Country**	**State**
TLC Plate	-	Merck Germany	-
Methanol CH_3OH	32.05	Synerlab, France	Liquid
Chloroform $CHCl_3$	119.38	Duksan reagent, Korean	Liquid
Hexane C_6H_{14}	86.18	RCI Labscan, Thailand	Liquid
Ethyl Acetate $CH_3COOC_2H_5$	88.11	RCI Labscan, Thailand	Liquid

Table 3. 6: Chemicals used in antioxidant activity determination

Chemical Name **Molecular Formula**	**Molecular Weight** **$gmol^{-1}$**	**Manufacturer** **Country**	**State**
2,2-Diphenyl-1-Picrylhydrazyl (DPPH) $C_{18}H_{12}N_5O_6$	394.32	TCI, Japan	Solid

Methanol CH_3OH	32.04	Synerlab, France	Liquid
Butylated hydroxyanisole $C_{11}H_{16}O_2$	180.24	Sigma-Aldrich, Germany	Solid

Table 3. 7: Chemical used in IR characterization of *N*-acylhydrazones

Chemical Name **Molecular Formula**	**Molecular Weight** **$gmol^{-1}$**	**Manufacturer** **Country**	**State**
Potassium Bromide KBr	119.00	Sigma-Aldrich, Germany	Solid

Table 3. 8: Chemical used in NMR characterization

Chemical Name **Molecular Formula**	**Molecular Weight** **$gmol^{-1}$**	**Manufacturer** **Country**	**State**
Dimethyl Sulfoxide-d_6 (DMSO-d_6) $(CD_3)_2SO$	78.13	Fisher Scientific, UK	Liquid

3.2 Instruments Used

Table 3. 9: Instruments used

Instrument	Manufacturer	Model
Nuclear Magnetic Resonance Spectrometer	Jeol	ECX-400
Melting Point Apparatus	Stuart	SMP 10
Fourier Transform Infrared Spectrometer	Perkin Elmer	Spectrum RX1
Rotary Evaporator	BUCHI	R-200
Ultrasonicator Bath	Bransonic	5510E-DTH
Ultraviolet–Visible Spectrophotometer	ThermoFisher	Genesys 50

3.3 Experimental Procedure

The synthesis of *N*-acylhydrazones involved multiple steps, which can be grouped into two main stages, described in detail below.

3.3.1 Synthesis of Carboxylic Acid Hydrazide

In the synthesis of carboxylic acid hydrazide, the hydrazone and ester would be synthesized before.

To synthesize the hydrazone, hydrazide hydrochloride was placed in a 250 mL round-bottom flask, followed by the dropwise addition of 130 mL of acetic acid was added into the flask to dissolve the reagents. 3 pieces of boiling chips and

magnetic stir bar were inserted into the flask. The flask was then immersed into an oil bath which is heated on a magnetic stirrer hotplate to start the overnight reflux process. The oil bath was heated to around 80 °C and the temperature was monitored by thermometer. The mixture was poured into crushed ice and stirred. The resulting phenylhydrazone was extracted with 100 mL of ethyl acetate twice. After the extraction process, the moisture in the ethyl acetate was removed by adding anhydrous magnesium sulphate and the ethyl acetate was removed by using the rotary evaporator, to obtain the hydrazone for following synthesis.

To synthesize ester, the obtained hydrazone from the previous step was kept in the 250 mL round-bottom flask with the addition of 2 mL of concentrated hydrochloric acid and 25 mL of absolute ethanol. The magnetic stir bar and boiling chips were also placed into the mixture. The reaction mixture was heated in the oil bath to around 80 °C to reflux for overnight. The mixture was poured into crushed ice, and the indole ester was extracted in 100 mL ethyl acetate twice. The collected ethyl acetate was dried with anhydrous magnesium sulphate and was removed by using rotary evaporator, to obtain the ester.

To synthesize the targeted compound, carboxylic acid hydrazide, the produced ester was kept in 250 mL round-bottom flask. 70 mL of hydrazine hydrate and 30 mL of absolute ethanol were added into the flask, followed by the insertion of boiling chips and magnetic stir bar. The mixture was refluxed overnight in the oil bath at around 80 °C. The reaction mixture was washed with crushed ice and extracted with 100 mL ethyl acetate twice. The moisture in the ethyl acetate was removed by

adding anhydrous magnesium sulphate and removed by using rotary evaporator to obtain carboxylic acid hydrazide.

After obtaining the carboxylic acid hydrazide, the purification was undergone by dissolving the crude carboxylic acid hydrazide in 95% ethanol by heating, followed by the filtration through the cotton wool. The filtrate was heated for concentrating and left it in room temperature to evaporate the solvent. The crude was then washed with cold ethanol and dried in the oven at 60 °C.

3.3.2 Synthesis of *N*-acylhydrazones

In the synthesis of a series of *N*-acylhydrazones, 2 mmol (0.4422 g) of synthesized carboxylic acid hydrazide was refluxed with 2mmol of corresponding benzaldehydes listed in **Table 3.10**:

Table 3. 10: Benzaldehydes Used in the Synthesis of *N*-acylhydrazones

Benzaldehyde	**Molecular Weight ($gmol^{-1}$)**	**2 mmol**	
		Mass (g)	**Volume (mL)**

4-Methylbenzaldehyde	120.15	-	0.236
2-Chlorobenzaldehyde	140.57	-	0.225
4-Chlorobenzaldehyde	140.57	0.2811	-
2,4-Dichlorobenzaldehyde	175.01	0.3500	-
3,4-Dichlorobenzaldehyde	175.01	0.3500	-
2-hydroxybenzaldehyde	122.12	-	0.211
4-hydroxybenzaldehyde	122.12	0.2442	-
4-Nitrobenzaldehyde	151.12	-	0.3022

2 mmol of the carboxylic acid hydrazide and 2 mmol of benzaldehyde with different substituent were added into a 100 mL round-bottom flask, followed by the addition of catalyst. The reactants were dissolved in 15 mL of absolute ethanol with the assistance of sonication. Three pieces of boiling chips and magnetic stir bar were inserted into the flask. The mixture was refluxed overnight in an oil bath at around 80 °C.

After the reflux process, the mixture was allowed to cool to room temperature and poured into crushed ice in a beaker. The mixture was stirred for a few minutes and left overnight to allow the precipitation. Vacuum filtration was utilized for the collection of crude product. During the filtration, the crude product was washed with distilled water to remove the residue of catalyst and unreacted reagent. Then, the collected crude product was dried overnight in an oven at 70 °C.

3.3.3 Recrystallization

The crude product was purified by utilizing recrystallization. The crude product weas dissolved in hot 95% ethanol and filtered through cotton wool stuffed in a glass filter funnel to another beaker. A few of boiling chips were added to both beakers to prevent the bumping. The solution was concentrated until the volume was reduced to 20 mL or the formation of solid and then removed from the hotplate. The solution was allowed to cool to room temperature and allowed the crystallization. The crystallized product was washed with minimum amount of cold ethanol and dried in an oven at 70 °C. The dried product was then weighed, and the percentage yield was calculated.

3.4 Characterization

Multiple analytical techniques, including melting point determination, NMR spectroscopy, FTIR spectroscopy, and TLC, were employed to characterize the products.

3.4.1 Melting Point Determination

The melting point of all synthesized compounds was measured to provide information on their purity and identity. A pure compound typically exhibits a narrow melting point range, whereas the presence of impurities results in a broader range.

Melting point measurements were performed using a melting point apparatus. A small quantity of the compound was placed into a capillary tube; the tube was then inserted into the apparatus. The temperature setting was adjusted up to 300 °C, as the compounds were expected to melt in the range of 220–280 °C. The temperature was increased gradually, and the temperatures at which the compound first began to melt and completely liquefied were recorded as the melting point range of the synthesized compound.

3.4.2 Nuclear Magnetic Resonance (NMR) Spectroscopy

Nuclear magnetic resonance (NMR) is a physical phenomenon arising from the magnetic properties of atomic nuclei when placed in a strong magnetic field. Based on this principle, NMR spectroscopy can provide physical, chemical, electronic, and structural information about molecules. Thus, NMR spectroscopy is a crucial analytical technique in organic chemistry, as it yields valuable insights into the chemical environment of specific nuclei within a molecule. Proton NMR (^{1}H NMR) and carbon-13 NMR (^{13}C NMR) are the most employed types of NMR analysis.

In the interpretation of ^{13}C NMR spectra, DEPT (Distortionless Enhancement by Polarization Transfer) was applied to distinguish the multiplicities of carbons, namely methyl, methylene, methine, and quaternary carbons. HMQC (Heteronuclear Multiple Quantum Correlation) spectroscopy was employed to establish direct one-bond correlations between protons and their attached carbons, while HMBC (Heteronuclear Multiple Bond Correlation) spectroscopy was used to identify long-range couplings between protons and carbons.

For sample preparation, about 25 mg of product was weighed into a clean sample vial and dissolved in a minimal volume of DMSO-d_6. The solution was transferred into an NMR tube to a sample height of approximately 4 cm from the bottom. The tube was then labelled and submitted for analysis.

3.4.3 Fourier Transform Infrared (FTIR) Spectroscopy

FTIR spectroscopy is an analytical technique used to identify the types of chemical bonds in a molecule. In the measurement of the absorption of infrared radiation, the important functional groups can be determined, as different bonds absorb at specific IR frequencies. Hence, FTIR spectroscopy was employed to identify the functional groups present in the synthesized compound.

Since anhydrous potassium bromide (KBr) does not absorb in the IR region and hence causes no interference, the solid sample was mixed with KBr in a ratio of approximately 1:10 and finely ground using a mortar and pestle. The homogenized

mixture was then pressed with a laboratory pellet press to form a pellet, which was placed in the FTIR spectrometer for scanning in the range of 4000 cm^{-1} to 400 cm^{-1}.

3.4.4 Thin Layer Chromatography (TLC)

Thin Layer Chromatography (TLC) is widely used in synthesis laboratories due to its simplicity, low cost, high sensitivity, and rapid results in testing purity as well as providing useful information for reaction monitoring. In this technique, the solvent serves as the mobile phase, while the TLC plate acts as the stationary phase. Based on the spots observed under an ultraviolet lamp, the purity of the compound can be assessed.

For the TLC analysis, a small quantity of the synthesized compound was dissolved in a clean sample vial with a minimal amount of methanol, followed by chloroform, and sonicated to ensure complete dissolution. The baseline and solvent front were drawn 1 cm from the bottom and top edges of the plate respectively. The sample was then spotted on the baseline using a capillary tube. To avoid overlapping, the distance between spots was maintained at approximately 1 cm, with each spot placed at least 0.5 cm from the edge of plate.

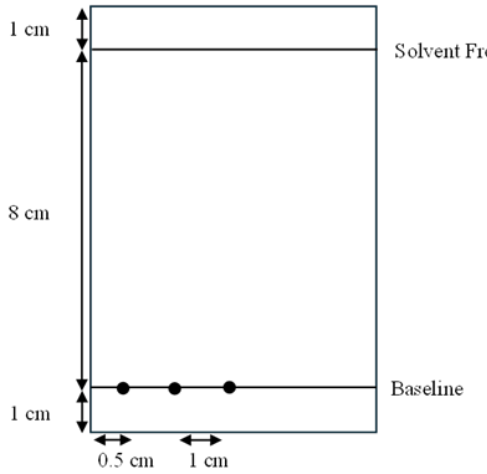

Figure 3. 1: TLC plate

The TLC plate was then placed in a developing chamber containing the mixture of hexane and ethyl acetate (1:1) as developing solvent. The plate was removed once the solvent reached the solvent front, and the solvent was allowed to evaporate. The developed spots were visualized under a UV lamp and marked with a pencil. The retardation factor (R_f) values were calculated for the observed spots.

3.5 Antioxidant Activity Determination

In the determination of the antioxidant activity of the synthesized *N*-acylhydrazones, the 1,1-diphenyl-2-picryl-hydrazyl (DPPH) assay, a convenient and effective method, was employed. DPPH is a stable free radical containing an unpaired electron on the bridging nitrogen atom. Due to the present of unpaired electron, the solution appears deep violet and exhibits strong absorption at 517 nm. When the DPPH radical is scavenged by an antioxidant, the violet solution turns yellow and the absorbance decreases. Thus, the antioxidant activity can be evaluated by

measuring the absorbance of mixture of DPPH and test compounds at 517 nm using an ultraviolet-visible (UV-Vis) spectrophotometer.

To prepare the DPPH solution, 3.8 mg of DPPH was dissolved in methanol in a 100 mL volumetric flask. The flask was immediately wrapped with aluminium foil, then shaken until the DPPH completely dissolved and incubated in the dark.

The antioxidant activity of a standard antioxidant, butylated hydroxyanisole (BHA), was first determined as a reference for comparison with the synthesized compounds. To prepare the BHA stock solution (500 ppm), 5 mg of BHA was dissolved in methanol in a 10 mL volumetric flask. A series of standard solutions with concentrations of 6.25 ppm, 12.5 ppm, 25 ppm, 50 ppm, 100 ppm, and 200 ppm were then prepared by serial dilution, starting from 200 ppm to ensure accuracy at lower concentrations. For each standard solution, 1 mL of solution was mixed with 4 mL of DPPH solution in a sample vial. The vial was immediately covered with aluminium foil and shaken vigorously for 1 minute. A blank solution, consisting of methanol and DPPH solution with same ratio (1:4) as standard solution was prepared. All mixtures were incubated in the dark for 30 minutes.

For the test samples, the same procedure was repeated by replacing BHA to synthesized compounds.

After incubation, the absorbance of each solution was measured at 517 nm using a UV–Vis spectrophotometer with methanol as the blank. Each absorbance value was measured three times, and the average absorbance was recorded to calculate the percentage of radical scavenging. The calibration curve of percentage radical

scavenging (y-axis) against concentration (x-axis) was constructed to determine the half maximal inhibitory concentration (IC_{50}). The entire measurement process was repeated twice more to obtain the average values and standard deviations.

3.6 Calculation

The following formulas were applied in the calculations:

- Mass of reagent needed:

  Mass (g) = number of moles (mol) × molecular mass (g/mol)

- Volume of reagent needed:

  $$\text{Volume (mL)} = \frac{\text{number of moles (mol)} \times \text{molecular mass (g/mol)}}{\text{density (g/mL)}}$$

- Yield percentage of product synthesized:

  $$\text{Yield percentage (\%)} = \frac{\text{experimental yield (g)}}{\text{theoretical yield (g)}} \times 100\%$$

- Retardation factor (R_f) of the substance:

  $$\text{Retardation factor} = \frac{\text{distance travelled by substance (cm)}}{\text{distance travelled by solvent (cm)}}$$

- Percentage of radical scavenging of the substance:

  $$\text{Percentage radical scavenging (\%)} = \frac{A_{blank} - A_{sample}}{A_{blank}} \times 100\%$$

  - A_{blank} = absorbance of blank solution
  - A_{sample} = absorbance of sample solution

CHAPTER 4

REUSLTS AND DISCUSSION

4.1 Molecular Structure of the Synthesized Compounds

In this project, carboxylic acid hydrazide and eight *N*-acylhydrazone derivatives, a total of nine compounds were synthesized. The compound codes, IUPAC names, and structures are presented in **Table 4.1**.

Table 4. 1: Code, name and structure of synthesized compound

4.2 Synthesis of Carboxylic Acid Hydrazide

In the synthesis of carboxylic acid hydrazide, the procedure can be divided into two parts, the generation of ester and the subsequent conversion to carboxylic acid hydrazide.

For the generation of ester, the process involves two steps. In the first step, condensation of starting materials is carried out in glacial acetic acid to yield the hydrazone intermediate. Acetic acid serves as both the solvent, provide an acidic

reaction medium, and as a mild, efficient catalyst that promotes the condensation (El-Sayed, Mahmoud and Hilgeroth, 2013). The mixture is refluxed at 80 °C and with stirring to maximize the reaction efficiency.

The second step involves cyclization of the hydrazone to obtain the moiety. The hydrazone is dissolved in absolute ethanol and concentrated hydrochloric acid is added as the catalyst. The reaction is conducted at the elevated temperature with stirring as previous. The hydrochloric is a strong acid that facilitates the tautomerization of arylhydrazone occurs to have ene-hydrazine, followed by a [3,3]-sigmatropic rearrangement to generate the intermediate which undergoes intramolecular cyclization. Protonation of the -NH- group, which is not involved in the ring formation, cause the leaving of NH_3, to form the moiety (Simoneau and Ganem, 2008).

Thus, in the condensation and cyclization part, different acids are employed for different purposes. Acetic acid provides a mild acidic medium without causing decomposition, while hydrochloric acid ensures the completion of the recyclization reaction.

After the generation of ester, it is reacted with hydrazine hydrate to yield the carboxylic acid hydrazide. The reaction proceeds via nucleophilic attack of the carbon of carbonyl group in the ester by the nitrogen of the hydrazine, which possesses a lone pair of electrons and acts as a nucleophile (Ouellette and Rawn, 2015). During this nucleophilic substitution, the ethoxy group, which originally bonded to the carbonyl carbon, serves as a good leaving group.

Thus, carboxylic acid hydrazide can be synthesized through this multistep pathway.

Scheme 4. 1: Synthetic route of carboxylic acid hydrazide

4.2.1 Discussion on Carboxylic Acid Hydrazide

At the room temperature, carboxylic acid hydrazide appears as light brown solid. The percentage yield is 31.08%. The melting point ranges from 176 to 179 °C. The retardation factor (R_f) is determined by thin layer chromatography (TLC) using a development solvent system of ethyl acetate and hexane (volume ratio = 1:1), and the measured R_f value is 0.075.

Table 4. 2: Physical properties of carboxylic acid hydrazide

Molecular weight (g/mol)	221.23
Appearance	Light brown solid
Percent yield (%)	31.08
Melting point (°C)	176-179
Retardation factor, R_f	0.075

According to the structure of carboxylic acid hydrazide (**Figure 4.1**):

Figure 4. 1: Structure of carboxylic acid hydrazide

The IR spectrum of carboxylic acid hydrazide exhibits several characteristic absorption bands. Strong peaks at 3326 and 3278 cm^{-1} correspond to N-H stretching vibrations. Medium intensity bands at 3067 and 2907 cm^{-1} are assigned to the

stretching vibrations of aromatic C-H and sp^3 C-H respectively. A strong and sharp absorption at 1676 cm^{-1} is attributed to the C=O stretching vibration, while an adjacent strong band at 1635 cm^{-1} is due to C=C stretching. The absorptions at lower wavenumbers that a peak at 1234 cm^{-1} assigned to C-N stretching, and a peak at 998 cm^{-1} corresponding to C-F stretching vibrations.

Table 4. 3: Summary of IR absorption bands for carboxylic acid hydrazide

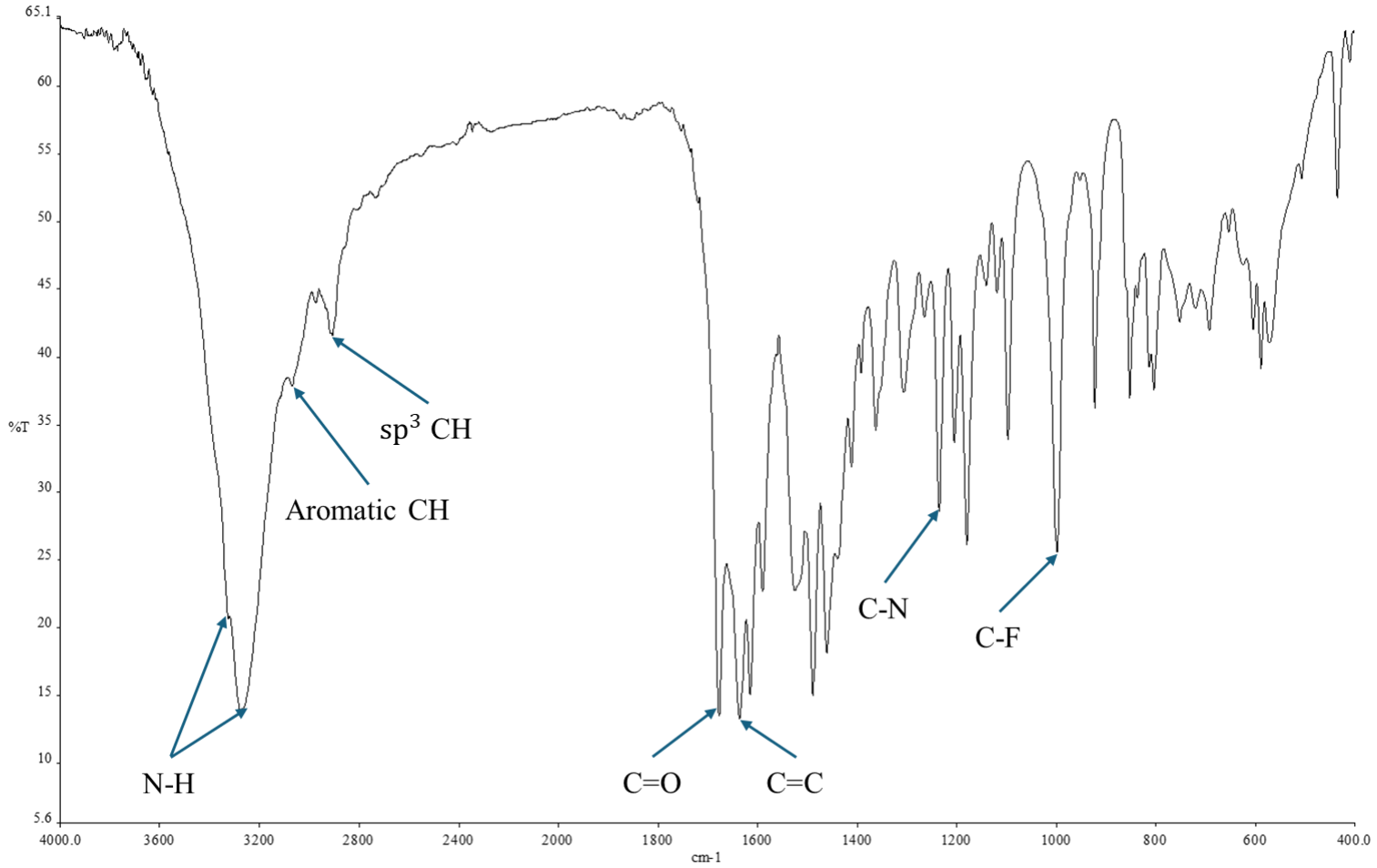

Figure 4. 2: IR spectrum of carboxylic acid hydrazide

The ^{1}H NMR spectrum of carboxylic acid hydrazide (**Figure 4.3**) exhibits two signals in the downfield region. A singlet peak at δ is assigned to the -NH- proton (H1) of the moiety, which is highly deshielded by the conjugated ring system, while another singlet peak at δ corresponds to the hydrazide -NH- proton (H10). In the aromatic region, δ 6.5-8 region (Cañada College, 2024), several multiplet signals are observed. In this range, a doublet of doublets (dd) at δ (*J*=10.4, 2.8 Hz), a doublet of doublets (dd) at δ (*J*=9, 4.6 Hz) and a triplet of doublets (td) at δ (*J*=9.1, 2.5 Hz) are assigned to H4, H7, and H6 respectively. A singlet peak at δ is attributed to the terminal -NH_2 protons (H11). In the upfield region, a singlet signal at δ attributable to the methylene group (H8) adjacent to the carbonyl, while a singlet signal at δ belonged to the methyl group.

In the ^{13}C spectrum (**Figure 4.4**), several peaks appear as doublets, which can be attributed to carbon-fluorine coupling (Skeel et al., 2020). Due to sp^2 hybridization and the presence of a carbon-oxygen double bond, the signal of the carbonyl carbon is deshielded to the furthest downfield, typically in the range of 170 to 220 ppm (Schaller et al., 2015). The signal observed at δ is assigned to carbonyl carbon (C9). In the aromatic region, doublet signals at δ, are attributed to C5, C3, C7, C6, C3, and C4, respectively, while the singlet signals at δ and δ are assigned to C2 and C7, respectively. In the upfield region, the peaks at δ correspond to methylene carbon (C8) and the methyl carbon, respectively. The methyl, methylene, methine and quaternary carbon were further distinguished by comparison of the ^{13}C NMR spectrum with DEPT 135 spectrum.

Furthermore, 2D NMR experiments, heteronuclear multiple quantum coherence (HMQC) and heteronuclear multiple bond correlation (HMBC), were utilized for the structural elucidation of carboxylic acid hydrazide. HMQC shows the correlations between carbons and their directly bonded protons (McKenzie et al., 2011). As a result, the assignment of proton and carbon signals can be further confirmed through the HMQC experiment. According to the HMQC spectrum of carboxylic acid hydrazide shown in **Appendix**, five correlation peaks were observed. Protons attached to nitrogen do not show correlations in HMQC, as they are not directly bonded to carbon.

The correlations between carbons and protons can also be observed in the HMBC experiment. However, HMBC does not display direct one-bond ^{13}C-^{1}H correlation but instead provides information on longer range couplings, typically two- or three-bond, and occasionally four-bond (Reynolds, 2016). For instance, in the HMBC spectrum of carboxylic acid hydrazide, the hydrogen shows the cross-peaks with C3 () and C2 (), which correspond to three-bond and two-bond correlations, respectively. However, no correlation is observed with the carbon of group to which the protons are directly bonded.

Therefore, by combining the results from various NMR experiments, the assignments of carbon and proton signals can be established.

Table 4. 4: Summary of ^{1}H and ^{13}C NMR spectral date of carboxylic acid hydrazide

Figure 4. 3: ^{1}H NMR (400 MHz, DMSO-d_6) spectrum of carboxylic acid hydrazide

Figure 4. 4: ^{13}C NMR (100 MHz, DMSO-d_6) spectrum of carboxylic acid hydrazide

4.3 Synthesis of *N*-acylhydrazones

After obtaining the key intermediate, carboxylic acid hydrazide, the desired *N*-acylhydrazones can be synthesized via a direct one-step reaction. Two reagents are involved in this synthesis, which are the prepared carboxylic acid hydrazide and corresponding aldehyde compounds. In this process, the nitrogen atom of hydrazide acts as a nucleophile and attacks the carbonyl carbon of aldehyde, leading to the formation of a C=N bond with the elimination of one molecule of water. Therefore,

the -C(=O)-NH-N=C- moiety is created through this nucleophile attack on carbonyl carbon.

In the reaction, acid serves as a catalyst. In addition to its environmentally friendly nature, acid is recognized as a highly effective and efficient catalyst for the condensation of aromatic aldehydes with amines in a methanolic system (Aboonajmi et al., 2014). Hence, this allows the reaction to proceed under mild conditions while affording good yields.

The general reaction scheme is illustrated as follows:

Scheme 4. 2: General reaction for the synthesis of *N*-acylhydrazones from carboxylic acid hydrazide and aldehydesv

4.3.1 Physical Properties of Synthesized *N*-acylhydrazones

Figure 4. 5: General chemical structure of *N*-acylhydrazones

In this project, a total of eight *N*-acylhydrazones (**SB 1-SB 8**) were synthesized successfully. The substituents (R) on the benzaldehyde ring for **SB 1** to **SB 8** are 4-CH_3, 2-Cl, 4-Cl, 2,4-Cl_2, 3,4-Cl_2, 2-OH, 4-OH, and 4NO_2, respectively. The yields range from 68.22% to 96.64%. Most of the compounds give yields above 72%, with the only exception being **SB 1**, which affords 68.22%. The relatively low yield of **SB 1** may be attributed to its fine powder form which increases sample loss during collection. The melting points fall within the range of 226-282 °C, with all compounds exhibiting narrow melting point ranges of 2-4 °C. Such narrow ranges indicate that the products are obtained in pure form. Melting point analysis provides reliable information for assessing purity. As even a very low concentration of impurities can depress the melting point and broaden the range. This occurs because eutectic phase formation always depresses the values of melting points. Most of the compounds are obtained as brown solid, except for **SB 8**, which appears as an orange solid. The retardation factor (R_f) values measured by TLC in the mixture of acetate and hexane (1:1) range from 0.181 to 0.456. Most compounds exhibit R_f value greater than 0.288, with exception of **SB 7**, which shows the lowest R_f value, 0.181. The low R_f value of **SB 7** may be attributed to its relatively high polarity, resulting in reduced mobility on the TLC plate.

Table 4. 5: Physical properties of *N*-acylhydrazones **SB 1-SB 8**

Compound	Percent yield (%)	Melting point (°C)	Physical appearance	Retardation factor
SB 1 (4-CH_3)	68	270-273	Light brown solid	0.319
SB 2 (2-Cl)	92	226-230	Light brown solid	0.450
SB 3 (4-Cl)	72	239-243	Light brown solid	0.300
SB 4 (2,4-Cl_2)	84	247-250	Brown solid	0.456
SB 5 (3,4-Cl_2)	93	232-234	Brown solid	0.350
SB 6 (2-OH)	77	245-247	Brown solid	0.356
SB 7 (4-OH)	73	240-242	Light brown solid	0.181
SB 8 (4-NO_2)	97	279-282	Orange solid	0.288

4.3.2 IR Characterizations of *N*-acylhydrazone SB 1-SB 8

The FTIR spectral data confirm the presence of functional groups in the synthesized *N*-acylhydrazones (**SB 1-SB 8**). The moiety is identified by strong N-H stretching absorptions at 3458-3182 cm^{-1}, intermediate aromatic C-H stretching bands at 3085-3043 cm^{-1}, sharp aromatic C=C absorptions at 1609-1552 cm^{-1}. The acylhydrazone moiety contributes to characteristic absorption bands at 1673-1656 cm^{-1} (strong, C=O stretching), 1648-1587 cm^{-1} (strong, C=N stretching), and a weak band at 1090-1030 cm^{-1} (C-N stretching). The N-H absorption overlaps with the indole N-H band in the 3458-3182 cm^{-1} region. The sp^3 C-H stretching vibrations of the methyl and methylene groups appear in the range of 2952-2878 cm^{-1}. Compounds **SB 2**, **SB 3**, **SB 4**, and **SB 5** display additional absorption bands at 799-786 cm^{-1}, consistent with C–Cl stretching. Due to the presence of hydroxyl substituents, **SB 6** and **SB 7** exhibit O-H absorption peaks at 3185 cm^{-1} and 3284 cm^{-1}, respectively. For **SB 8**, which contains a nitro group, strong absorptions corresponding to the asymmetric and symmetric N-O stretching vibrations are observed at 1517 cm^{-1} and 1340 cm^{-1}, respectively.

Table 4. 6: Summary of IR spectral date for *N*-acylhydrazones **SB 1- SB 8**

Compound	N-H	O-H	Aromatic C-H	sp^3 C-H	C=O	C=N	Aromatic C=C	N-O	C-N	C-Cl
SB 1	3296 & 3202	-	3058	2919	1660	1607	1560	-	1071	-
SB 2	3298 & 3238	-	3064	2907	1669	1648	1593	-	1049	797
SB 3	3290 & 3197	-	3053	2900	1656	1604	1588	-	1075	795
SB 4	3310 & 3234	-	3055	2909	1673	1587	1552	-	1048	786
SB 5	3302 & 3182	-	3047	2919	1659	1589	1560	-	1030	799
SB 6	3458	3185	3043	2878	1665	1618	1587	-	1033	-
SB 7	3412	3284	3058	2917	1656	1640	1609	-	1069	-
SB 8	3402	-	3085	2952	1667	1609	1578	1517 & 1340	1090	-

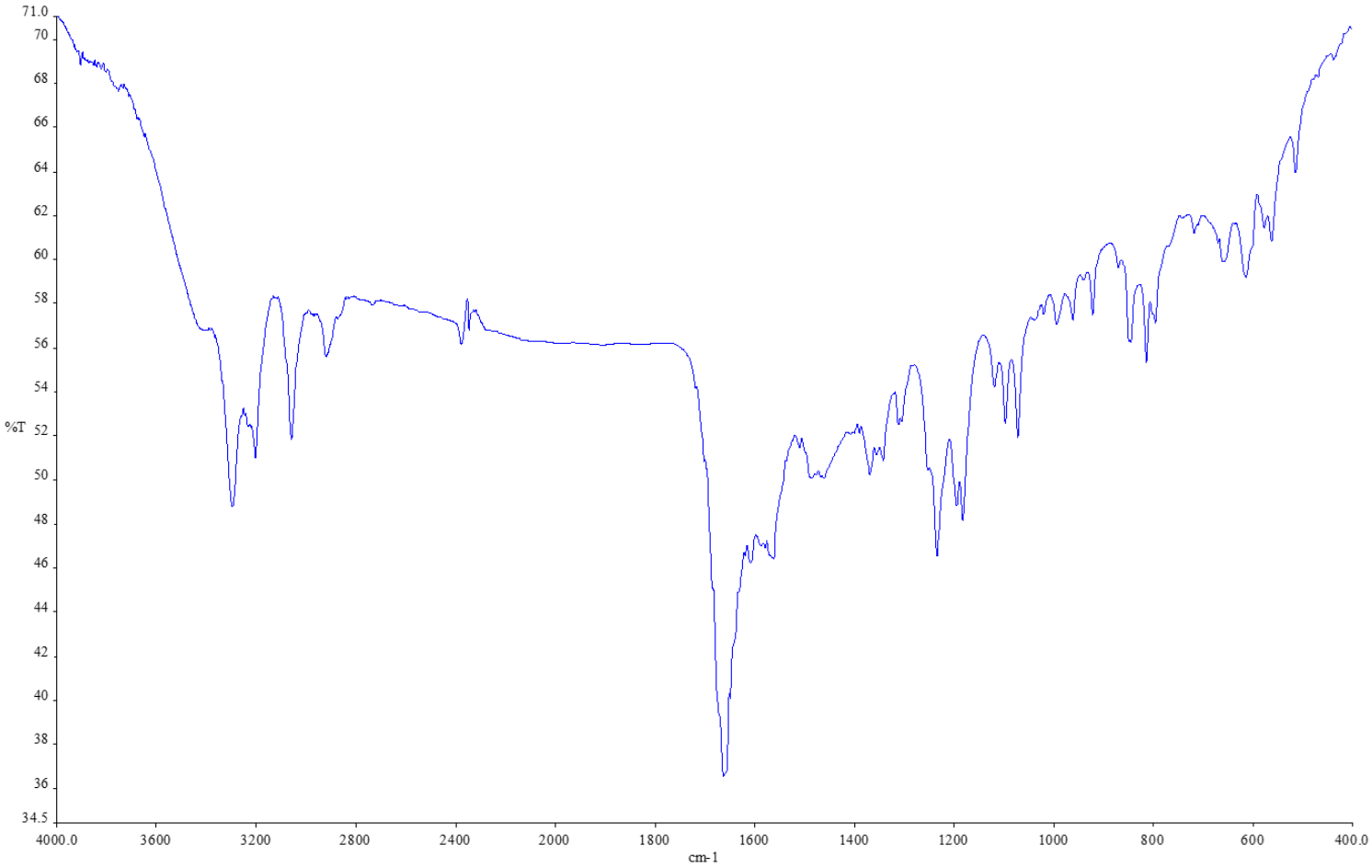

Figure 4. 6: IR spectrum of **SB 1**

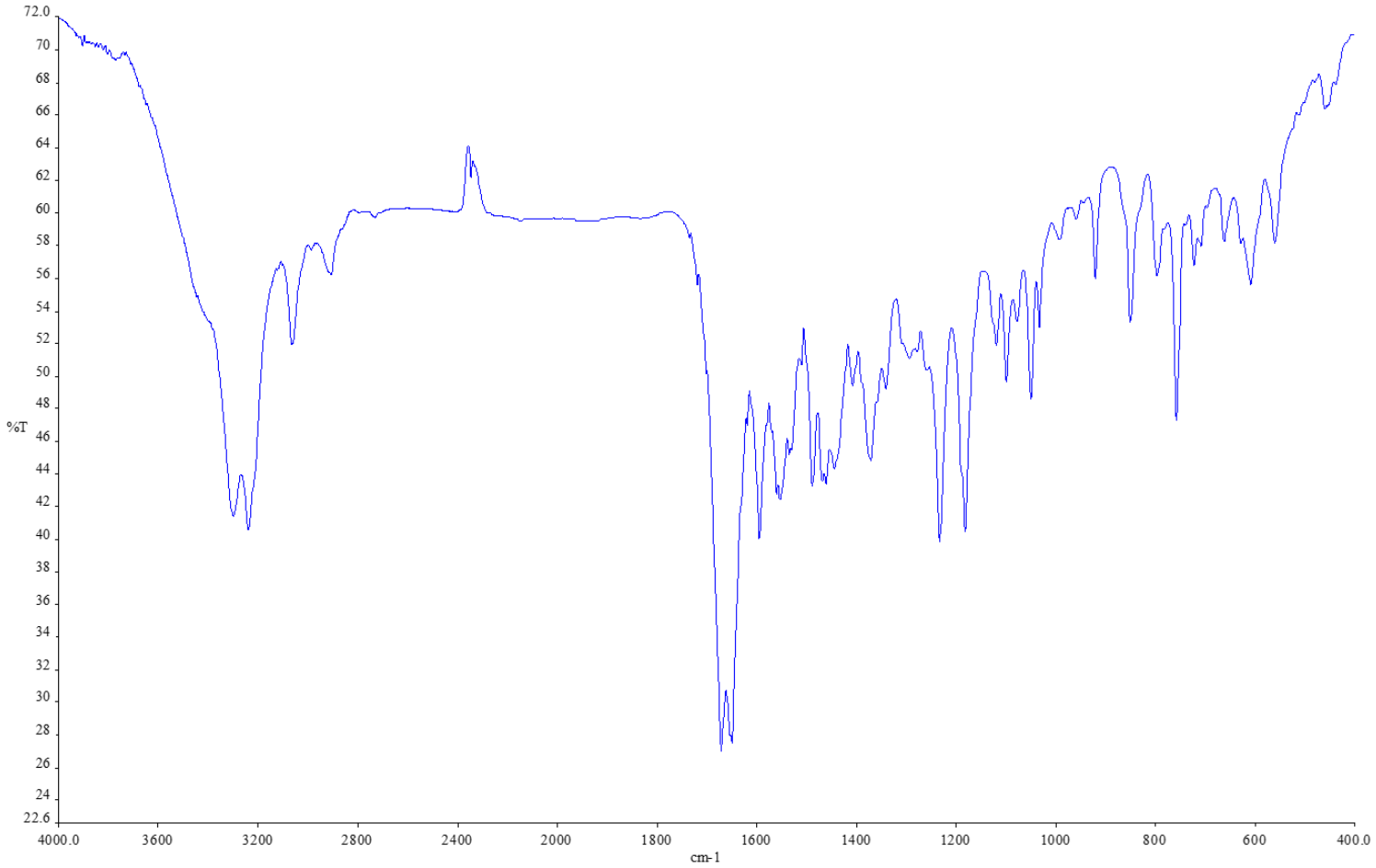

Figure 4. 7: IR spectrum of **SB 2**

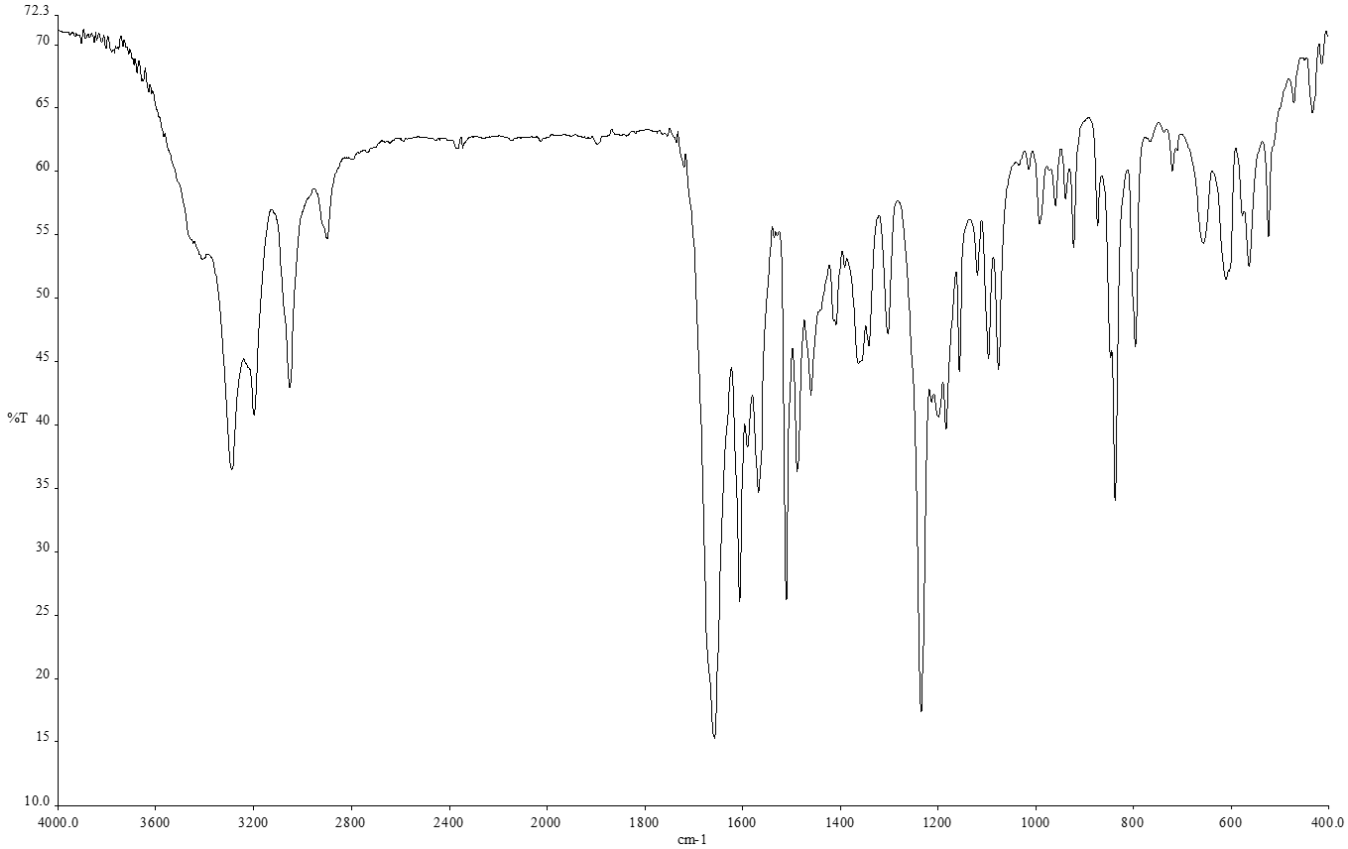

Figure 4. 8: IR spectrum of **SB 3**

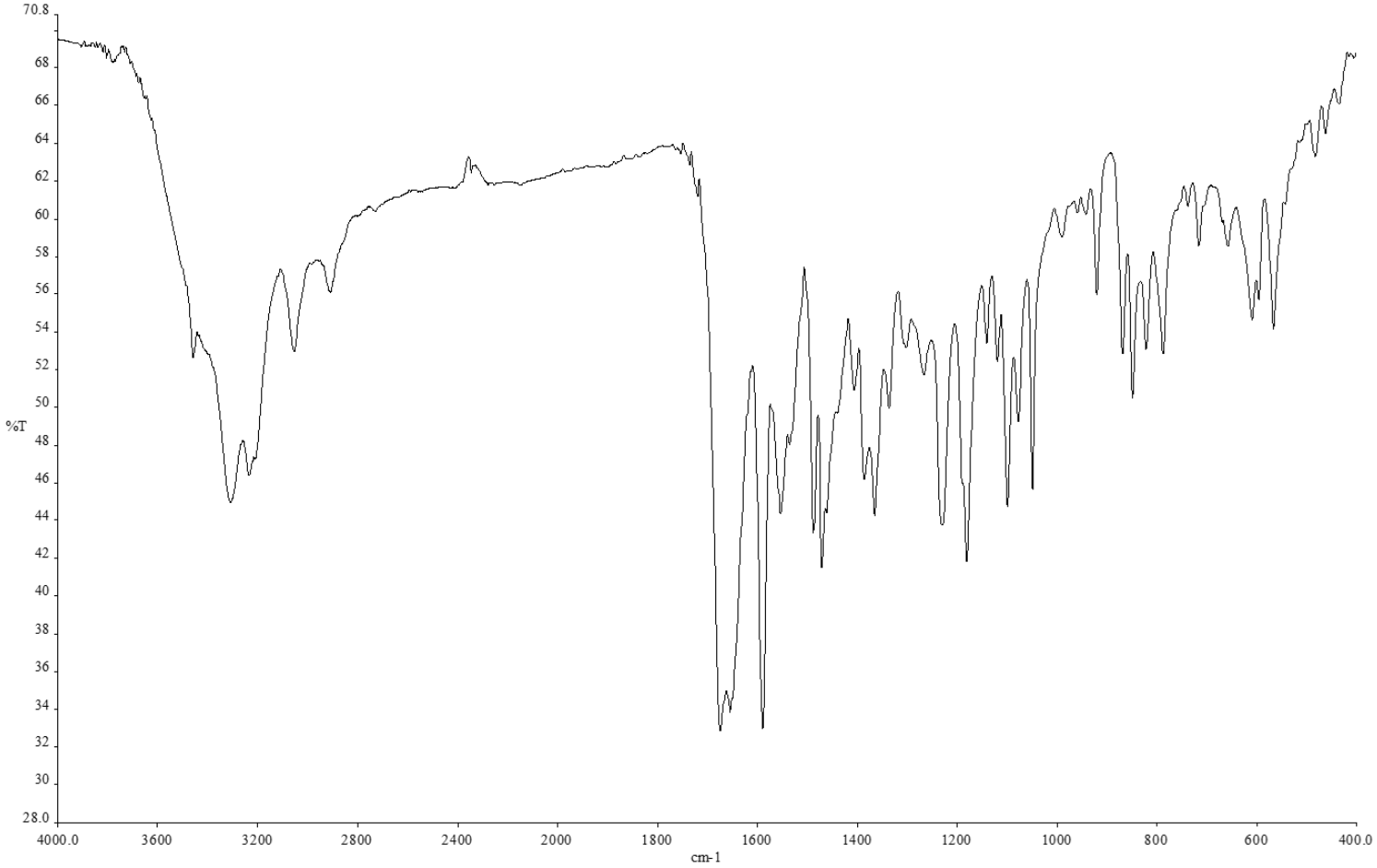

Figure 4. 9: IR spectrum of **SB 4**

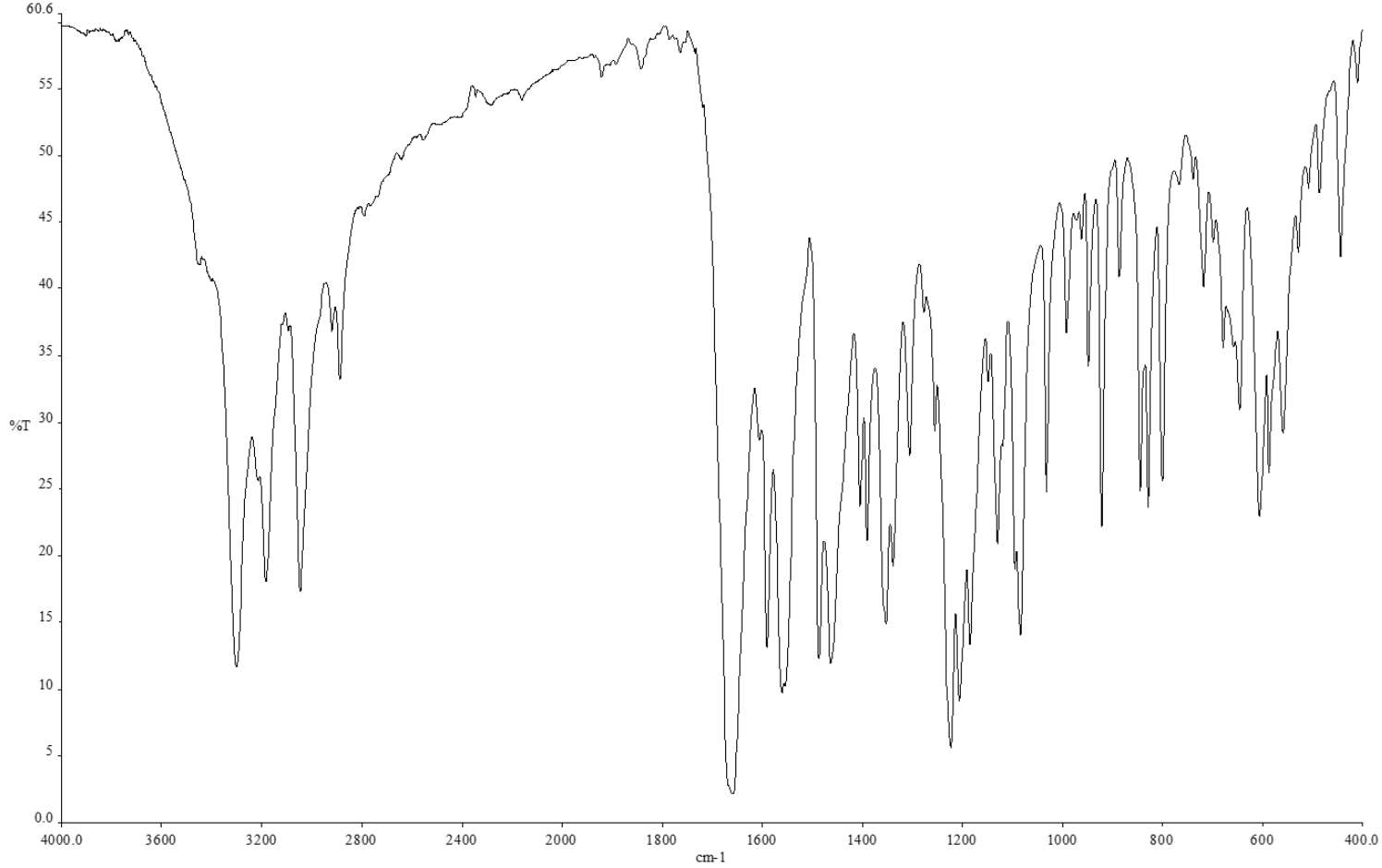

Figure 4. 10: IR spectrum of **SB 5**

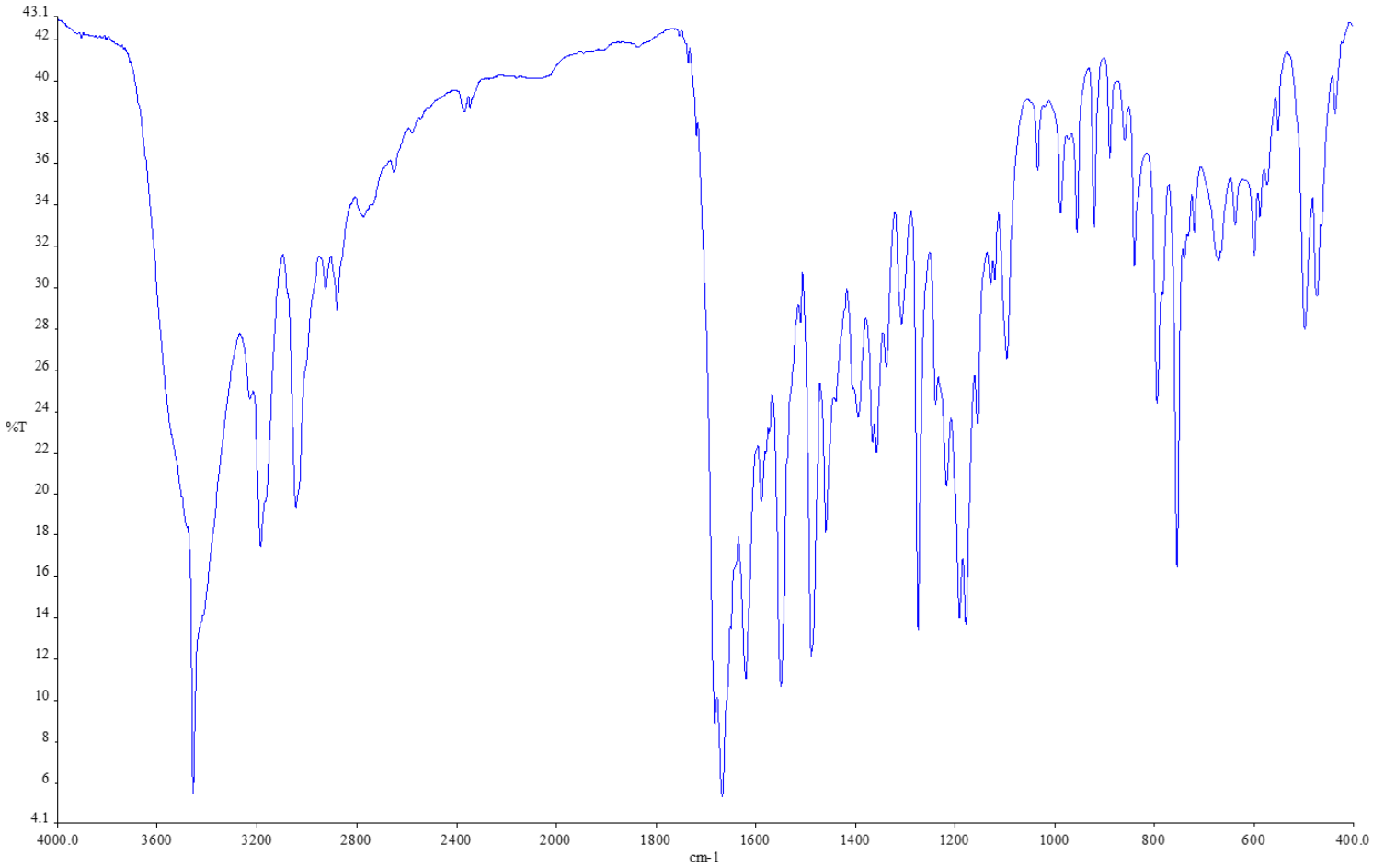

Figure 4. 11: IR spectrum of **SB 6**

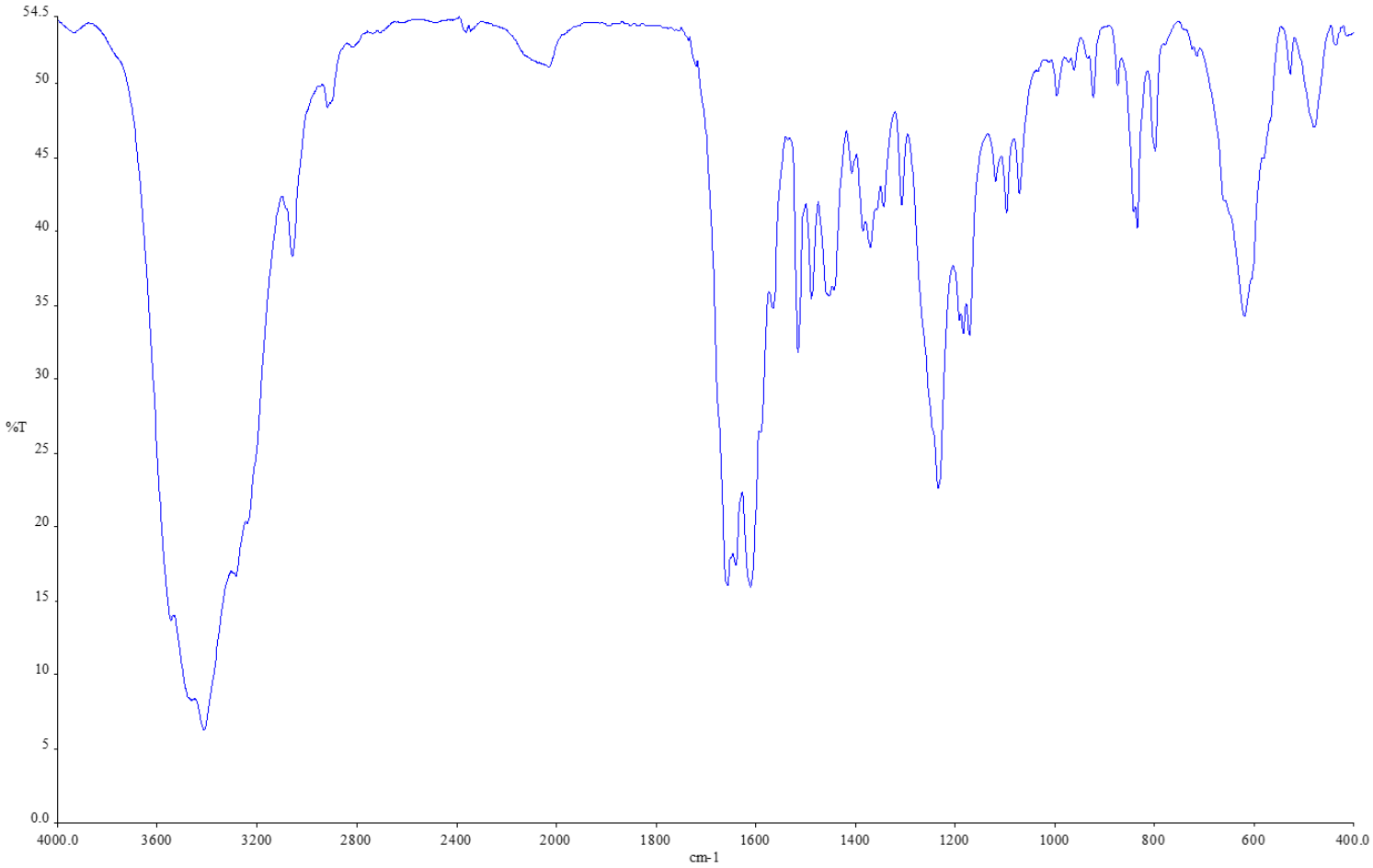

Figure 4. 12: IR spectrum of **SB 7**

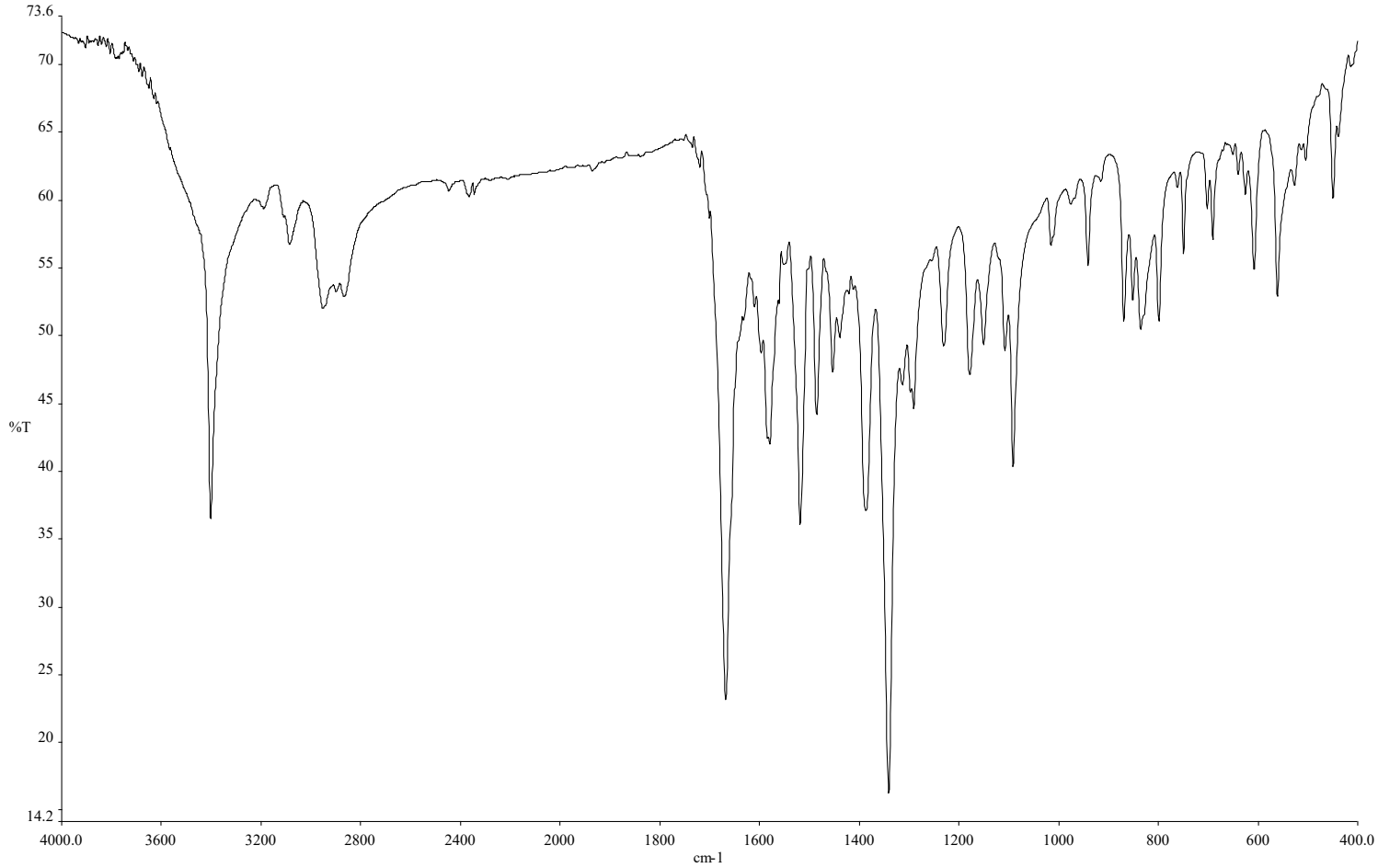

Figure 4. 13: IR spectrum of **SB 8**

4.3.3 NMR Structural Characterizations of *N*-acylhydrazones

In this project, a total of eight *N*-acylhydrazones were successfully synthesized and their chemical structure was elucidated using various NMR experiments. Based on the spectral information from ^{1}H NMR, ^{13}C NMR, DEPT 135, HMQC and HMBC studies, the formation of compounds **SB 1-SB 8** was confirmed.

Figure 4. 14: General chemical structure of **SB 1-SB 8** (**Figure 4.5**)

Due to presence of acyl moiety, the compounds exhibit both geometric and conformational isomerism. However, in this project, only the *E* isomer was synthesized, which will be discussed at later part (**Chapter 4.3.4.2**). For conformational isomerism, *cis* and *trans* isomers existed in all the compounds due to presence of two distinct sets of signals in the ^{1}H and ^{13}C spectra.

To distinguish these conformers, the chemical shift of amide proton (H10) was used. Previous studies (Hamzi, Barhoumi-Slimi and Abidi, 2016; Lopes et al., 2013) have reported that the amide proton of *trans* conformer is more deshielded, and hence, the signal appears at a relatively downfield position compared to the *cis* conformer.

After confirming the *cis* and *trans* signals of the amide proton, the remaining signals corresponding to the two conformers can be distinguished based on peak

intensity. Once the intensity of the amide proton signals is determined, this information can be used to differentiate between the *cis* and *trans* conformers, as the integral values reflect the ratio of each conformer in the compound (Ando et al., 2000). All proton signals arising from the same conformer should exhibit consistent relative intensities. For instance, if the amide proton of the *cis* conformer shows a more intense signal, then the other proton signals corresponding to the *cis* conformer will also appear more intense than those of the *trans* conformer.

The population of *cis* and *trans* conformer will also be discussed at later (**Chapter 4.3.4.1**). In the synthesized compounds, most of them exhibit a greater *cis* population than *trans* and thus show greater *cis* signal intensity. However, an exception is observed in **SB 6**, which bears a hydroxyl group at position 2'. It shows a more intense *trans* peak than *cis*, indicating that the trans conformer is more populated in this compound. This suggests that the presence of the hydroxyl group may influence the conformation equilibrium.

In the 1H NMR spectrum, nonaromatic protons are generally observed in the upfield region, whereas protons attached to nitrogen appear in the downfield region due to the greater deshielding effect. The signal corresponding to the protons of the indole moiety and benzaldehyde aromatic ring are typically located between 6 to 9 ppm. Within each group, the indole protons exhibit similar chemical shifts, and likewise, the benzaldehyde protons show comparable chemical shifts.

Similar chemical shift trends to those observed in the ^{1}H spectrum are also found in the ^{13}C spectrum. When the coupling constant is large, the signal may be

misinterpreted as two different peaks. Therefore, it is essential to recognize the coupling to avoid misinterpretation.

For further discussion, **SB 1** is selected as the representative compound.

4.3.3.1 ^{1}H NMR Structural Characterizations of *N*-acylhydrazones

In the ^{1}H NMR spectrum, a total of 11 proton signals are observed. The methyl and methylene protons resonate at upfield region, are assigned to 4'-CH_3, CH_3 and H8, respectively.

In the aromatic region, the doublet of doublets at is assigned to H6, while the doublet at corresponds to H2' & 6'. Other proton signals are observed for H7, H4 and H3' & 5', respectively.

In the downfield region, signals are observed at which are attributed by H12, H1 and H10 respectively. H12 is bonded to imine carbon, experiences a stronger deshielding effect. H10 and H1 are protons attached to nitrogen atoms of the amide and indole respectively, and hence are more deshielded, appear at higher chemical shift.

Figure 4. 15: 1H NMR spectrum of **SB 1**

4.3.3.2 ^{13}C NMR Structural Characterizations of *N*-acylhydrazones

In the ^{13}C NMR spectrum of **SB 1**, 17 signals are observed, although the compound contains 19 carbons. This reduction arises from molecular symmetry, hence C2' and C3' resonate at the same chemical shift as C6' and C5', respectively.

The peaks are classified as quaternary, methine, methylene and methyl carbons using the DEPT 135 experiment. In the DEPT 135 spectrum, quaternary carbons are absent, methine and methyl carbons appear as positive signals, and methylene carbon appears as negative signal. The assignments are further supported by corelations observed in HMQC and HMBC.

In the upfield region, the signals for CH_3, 4'-CH_3, and C8 appear respectively. For the moiety, the signals are attributed to C4, C3, C6, C7, C3, C7, and C2, respectively. The benzaldehyde carbons observed at are assigned to C2'&6', C3'&5', C1' and C4', respectively. In the downfield region, the signals at correspond to C12, C5 and C9, respectively.

Figure 4. 16: ^{13}C NMR spectrum of **SB 1**

4.3.3.3 NMR Structural Characterization of SB 1

Figure 4. 17: Chemical structure of **SB 1**

Table 4. 7: Summary of ^{1}H and ^{13}C spectral information of **SB 1**

4.3.3.4 NMR Structural Characterization of SB 2

Figure 4. 18: Chemical structure of **SB 2**

Table 4. 8: Summary of ^{1}H and ^{13}C spectral information of **SB 2**

4.3.3.5 NMR Structural Characterization of SB 3

Figure 4. 19: Chemical structure of **SB 3**

Table 4. 9: Summary of ^{1}H and ^{13}C spectral information of **SB 3**

4.3.3.6 NMR Structural Characterization of SB 4

Figure 4. 20: Chemical structure of **SB 4**

Table 4. 10: Summary of ^{1}H and ^{13}C spectral information of **SB 4**

4.3.3.7 NMR Structural Characterization of SB 5

Figure 4. 21: Chemical structure of **SB 5**

Table 4. 11: Summary of ^{1}H and ^{13}C spectral information of **SB 5**

4.3.3.8 NMR Structural Characterization of SB 6

Figure 4. 22: Chemical structure of **SB 6**

Table 4. 12: Summary of ^{1}H and ^{13}C spectral information of **SB 6**

4.3.3.9 NMR Structural Characterization of SB 7

Figure 4. 23: Chemical structure of **SB 7**

Table 4. 13: Summary of ^{1}H and ^{13}C spectral information of **SB 7**

4.3.3.10 NMR Structural Characterization of SB 8

Figure 4. 24: Chemical structure of **SB 8**

4.3.4 Conformational Studies of *N*-acylhydrazones

As mentioned in the introduction, the acylhydrazone moiety consists of amide [C(=O)-NH] and imine (C=N) function groups, which contribute to both geometric (*E/Z*) and conformational (*cis/trans*) isomerism. Theoretically, *N*- acylhydrazones should exhibit four difference isomers, which are the *cis/trans* conformers of both the *E/Z* geometric isomers. However, studies have shown that *N*- acylhydrazones exist only as *cis/trans* conformers of the *E* geometrical isomer (Munir et al., 2021).

The E isomer predominates over Z isomer due to its superior stability, which arises from reduced steric hindrance in this geometric position.

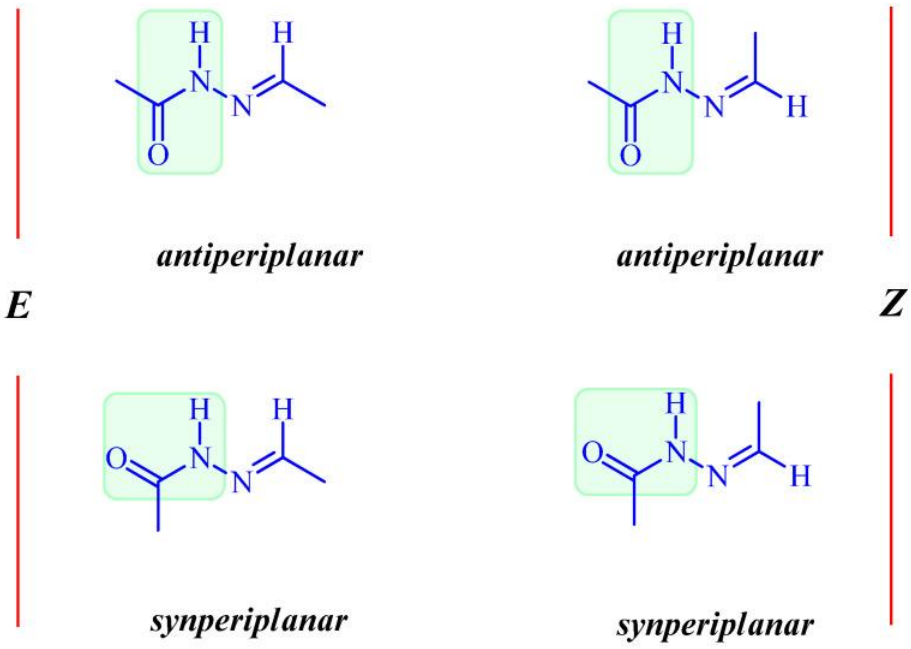

Figure 4. 25: Four possible isomers of *N*-acylhydrazones (same as **Figure 1.14**)

4.3.4.1 Conformation of CO-NH bond of *N*-acylhydrazones

The ratio of the amide *cis/trans* conformer can be determined from the integration values of their respective signals in the ^{1}H NMR spectrum. The H10 proton, which is attached to the amide nitrogen, is selected for this calculation. H10 is selected because its signals are observed in the highly downfield region, and their assignment has been well supported by many studies. In the studies, the *trans*

conformer consistently appears further downfield than the *cis* conformer, while the *cis* conformer typically shows greater peak intensity than the *trans*. Therefore, H1 is a relatively simple and reliable proton for *cis/trans* conformer ratio calculation.

The ^{1}H spectrum of **SB 1** is used here to demonstrate the calculation.

Figure 4. 26: ^{1}H NMR spectrum of **SB 1** - NH region and integration

According to the integration values shown in **Figure 4.**, the percentage of the *cis* and *trans* conformers can be calculated using following formula.

$$\%\ cis = \frac{cis}{cis + trans} \times 100\% \qquad \%\ trans = \frac{trans}{cis + trans} \times 100\%$$

The percentage of *cis* and *trans* conformers of **SB 1-SB 8** are summarized in **Table 4.14**.

Table 4. 14: Percentages of cis and trans conformers

Most of the compounds exhibit a higher proportion of the *trans* conformer compared to the *cis* conformer, with *trans:cis* ratios of 2:2.78 (**SB 1-SB 5** and **SB 7**) and 2:2.94 (**SB 8**) which are comparable to the reported value of 2: 3 (Kumar et al., 2017). The exception is SB 6 which contains a hydroxyl group at the carbon position 2 of benzaldehyde and shows a greater amount of the *trans* conformer than *cis* conformer.

Figure 4. 27: Chemical structures of *cis* and *trans* conformer of **SB 6**

According to the chemical structures (**Figure 4.27**), the hydroxyl group in the *trans* conformer is closer to the carbonyl oxygen than in the *cis*, resulting in the formation of an intramolecular hydrogen bond. This intramolecular hydrogen bond restricts rotation and provides greater stability against conformational changes (Boros et al., 2017). Hence, **SB 6** is the only compound that has a greater quantity of the *trans* conformer than the *cis* conformer.

4.3.4.2 Geometric Isomerism of *N*-acylhydrazones

Differential Nuclear Overhauser Effect (NOE) experiments were used to determine the geometric isomerism of *N*-acylhydrazones across the imine (C=N) bond. **SB 1** is selected as a representative compound for discussion.

According to the differential NOE spectra of compound **SB 1**, the NOE enhancement of the imine proton (H12) was observed upon irradiation of the imide proton (H10). Furthermore, irradiation of the imine proton (H12), NOE enhancements were detected for H10 and H2'. Similar results were observed for the other compounds (**SB 2-SB 8**). Therefore, based on the differential NOE spectra, the presence of the *E* isomer is strongly suggested in compounds **SB 1-SB 8**.

Figure 4. 28: Differential NOE spectrum of **SB 1**, irradiated at 11.18 ppm

Figure 4. 29: Differential NOE spectrum of **SB 1**, irradiated at 7.94 ppm

4.3.4.3 Rotational Barriers around the CO-NH Bond for *N*-acylhydrazones

Dynamic NMR experiments were employed to determine the rotational energy barriers between *cis* and *trans* isomers of the synthesized *N*-acylhydrazones. Compound **SB 1** was chosen as a model compound for discussion.

The coalescence of the amide NH proton (H10) is observed with increasing temperature, as demonstrated in the following dynamic NMR spectrum:

Figure 4. 30: Dynamic NMR spectrum of **SB 1**

The coalescence temperature (T_c) of the amide proton (H10) peak of compound **SB 1** was determined to be 363 K. Besides T_c, the peak separation ($\Delta\nu$, in Hz) is also required to calculate the rate constant (k_c), which indicates the rate of *cis/trans* conformers exchange. The $\Delta\nu$ value between the *cis* and *trans* peaks of H10 was

measured prior to signal coalescence. To convert the unit from ppm to Hz, the chemical shift difference (ppm) is multiplied by the spectrometer frequency (400 MHz). With T_c and $\Delta\nu$ obtained, k_c can then be calculated using the rate constant equation: $k_c = (\pi \times \nu)/2^{1/2}$.

By rearranging the Eyring equation ($k_c = \frac{k_c T_c}{h} e^{\frac{-\Delta G^{\ddagger}}{RTc}}$), the expression for calculating the Gibbs free energy of activation in kJ/mol can be obtained: $\Delta G^{\ddagger} = 19.14Tc\ (10.32+\log Tc/kc) \times 10^{-3}$.

The rotational barrier is determined from the Gibbs free energy of activation. The Gibbs free energies of activation of **SB 1-SB 8** are summarized in **Table 4.15**.

Table 4. 15: Summary of Gibbs Free Energies of Activation of **SB 1-SB 8**

The comparable Gibbs free energy of activation values indicate that all synthesized compound exhibits similar rotational barriers.

4.4 Antioxidant Activity Evaluation of *N*-acylhydrazones

The antioxidant activity of **SB 1-SB 8** was evaluated using DPPH assay. DPPH is a stable free radical that exhibits a deep purple colouration. When it accepts an electron from an antioxidant, the radical is scavenged, leading to a fading of the purple colour. The DPPH solution shows a strong absorbance at 517 nm, and this absorbance decreases, upon accepting an electron from antioxidant (Baliyan et al.,

2022). Therefore, the antioxidant activity of a compound can be evaluated by referring the absorbance value through UV-Vis spectrophotometry.

Before determining the antioxidant activity of the synthesized compounds (**SB 1-SB 8**), the IC_{50} value of the standard antioxidant, butylated hydroxyanisole (BHA) was first measured. BHA is a synthetic antioxidant, commonly used as a reference, to compare the antioxidant activity of tested compounds against DPPH radical (Shahidi and Zhong, 2015).

The IC_{50} value of BHA is 0.94 ± 0.17 µM.

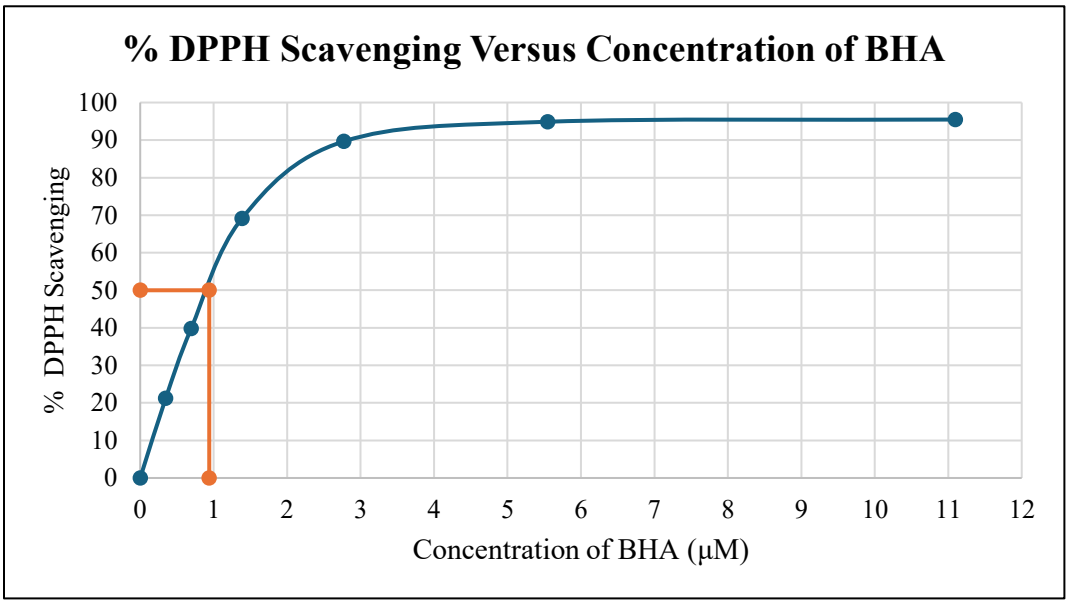

Figure 4. 31: Graph of % DPPH scavenging versus concentration of BHA

The synthesized compounds did not show the properties of antioxidant, as the absorbance of DPPH remained unchanged across varying sample concentrations. Among the compounds, only **SB 7** showed a slight decrease in absorbance with increasing concentration. However, comparing with BHA, the antioxidant activity of **SB 7** is insignificant can be considered as negligible.

The insignificant antioxidant activity observed may be attributed to the limited presence of phenolic hydroxyl groups (Charlton et al., 2023). The strong natural antioxidants such as tannins and gallic acid, contain a high number of phenolic hydroxyl group. As mentioned above, **SB 7** is the only synthesized compound exhibits potential of antioxidant activity, which can be correlated to the existence of a hydroxyl group at position 4'. Phenolic OH groups play a crucial role in antioxidant activity, as they can donate a hydrogen atom to neutralize reactive radicals and stabilize themselves through electron delocalization within the aromatic ring system. However, **SB 6,** which also bears OH group but at position 2', did not show similar antioxidant activity. This may be due to intramolecular interactions that hinder hydrogen donation. Therefore, to enhance antioxidant activity, the introduction of additional hydroxyl groups into the aromatic ring system should be considered.

In addition, the relatively low degree of conjugation in the synthesized compound may also contribute to the lack of antioxidant activity. Effective antioxidant must be capable to stabilize themselves after donating an electron to a reactive oxidant. Compounds with highly conjugated systems can delocalize electron more effectively (Bonner and Arbiser, 2014). As noted in the introduction, coumarin *N*-acylhydrazones, which exhibit the antioxidant activity, possess such extended conjugation. Thus, in addition to phenolic hydroxyl groups, the presence pf a conjugated system is also an important factor influencing the antioxidant properties of the synthesized compounds.

CHAPTER 5

CONCLUSION

5.1 Conclusion

In this project, a total of eight new *N*-acylhyrdrazone derivatives (**SB 1-SB 8**) bearing an moiety were successfully synthesized through the condensation of carboxylic acid hydrazide and various benzaldehydes. The compounds were obtained in the yields ranging from 68% to 97%. The compounds were characterized by physical methods, including melting point and physical appearance, as well as by spectroscopic techniques, such as FTIR, ^{1}H NMR, ^{13}C NMR, DEPT 135, HMQC and HMBC.

The *E/Z* isomerism of the synthesized *N*-acylhyrazone derivatives was confirmed by differential NOE. The results indicated that all compounds exist exclusively as the *E* isomer. The relative population of *cis* and *trans* conformers were determined by the integration of the amide proton signals in the ^{1}H NMR spectra, revealing *cis* conformer contents between 31.97% to 59.52% and *trans* conformer contents between 40.48% to 68.03%. Most compounds were found to exist predominantly in *cis* conformer, except for compound **SB 6,** which exhibits a higher proportion of the *trans* conformer. Dynamic NMR experiments were employed to investigate the

rotational barrier between the two conformers, giving Gibbs free energy of activation values ranging from 73.47 kJ/mol to 77.81 kJ/mol.

The antioxidant activity of the synthesized *N*-acylhydrazone derivatives was evaluated using DPPH assay with BHA (IC_{50}=0.94 ± 0.17 μM) as the reference standard. None of the compounds exhibited significant oxidant activity, although compound **SB 7** showed slight potential.

5.2 Further Studies

N-acylhydrazone derivatives have been widely reported in the literature to exhibit diverse biological activities, including antimalarial, antibacterial, anticancer and antitumour properties. With respect to antioxidant activity, structural modifications such as the incorporation of additional hydroxyl groups into the aromatic ring and the enhancement of conjugation may enhance the radical scavenging capability.

For further characterization, the synthesized compounds can be analysed by mass spectrometry to determine their mass-to-charge ratios (*m/z*). In addition, CHN elemental analysis can be employed to confirm the carbon, hydrogen, and nitrogen contents of the compounds.

REFERENCES

Aboonajmi, J., Maghsoodlou, M.T., Hazeri, N., Lashkari, M. and Kangani, M. (2014). 'Tartaric acid: a natural, green and highly efficient catalyst for the one-pot synthesis of functionalized piperidines', *Research on Chemical Intermediates*, 41(11), pp. 8057–8065. Available at: https://doi.org/10.1007/s11164-014-1877-1.

Aboul-Fadl, T., Abdel-Aziz, H.A., Kadi, A., Bari, A., Ahmad, P., Al-Samani, T. and Ng, S.W. (2011). 'Microwave-assisted one-step synthesis of fenamic acid hydrazides from the corresponding acids', *Molecules*, 16(5), pp. 3544–3551. Available at: https://doi.org/10.3390/molecules16053544.

Ando, I., Kobayashi, M., Kanekiyo, M., Kuroki, S., Ando, S., Matsukawa, S., Kurosu, H., Yasunaga, H. and Amiya, S. (2000). 'Chapter 4 - NMR spectroscopy in polymer science', in Toyoichi Tanaka *Experimental methods in polymer science*. Elsevier, pp. 261–493. Available at: https://doi.org/10.1016/b978-0-08-050612-8.50010-6.

Aykul, S. and Martinez-Hackert, E. (2016). 'Determination of half-maximal inhibitory concentration using biosensor-based protein interaction analysis', *Analytical Biochemistry*, 508(2016), pp. 97–103. Available at: https://doi.org/10.1016/j.ab.2016.06.025.

Baliyan, S., Mukherjee, R., Priyadarshini, A., Vibhuti, A., Gupta, A., Pandey, R.P. and Chang, C.-M. (2022). 'Determination of antioxidants by DPPH radical

scavenging activity and quantitative phytochemical analysis of Ficus Religiosa', *Molecules*, 27(4), article number 1326. Available at: https://doi.org/10.3390/molecules27041326.

Barresi, E., Baglini, E., Poggetti, V., Castagnoli, J., Giorgini, D., Salerno, S., Taliani, S. and Settimo, F.D. (2024). 'Indole-based compounds in the development of anti-neurodegenerative agents', *Molecules*, 29(9), article number 2127. Available at: https://doi.org/10.3390/molecules29092127.

Bonner, M.Y. and Arbiser, J.L. (2014). 'The antioxidant paradox: what are antioxidants and how should they be used in a therapeutic context for cancer', *Future Medicinal Chemistry*, 6(12), pp. 1413–1422. Available at: https://doi.org/10.4155/fmc.14.86.

Boros, E., Srinivas, R., Kim, H., Raitsimring, A.M., Astashkin, A.V., Poluektov, O.G., Niklas, J., Horning, A.D., Tidor, B. and Caravan, P. (2017). 'Intramolecular hydrogen bonding restricts Gd–aqua-ligand dynamics', *Angewandte Chemie International Edition*, 56(20), pp. 5603–5606. Available at: https://doi.org/10.1002/anie.201702274.

Boubekri, Y., Slassi, S., Aarjane, M., Tazi, B. and Amine, A. (2024). 'Microwave assisted synthesis, photoisomerization study and antioxidant activity of a series of *N*-acylhydrazones', *Arabian Journal of Chemistry*, 17(9), pp. 105913–105913. Available at: https://doi.org/10.1016/j.arabjc.2024.105913.

Cañada College (2024). *2.9: Spectroscopy of aromatic compounds*. Available at: https://chem.libretexts.org/Courses/can/CHEM_232_Organic_Chemistry_II_(Puenzo)/02%3A_Benzene_and_Aromaticity/2.09%3A_Spectroscopy_of_Aromatic_Compounds (Accessed 8 Sep. 2025).

Charlton, N.C., Mastyugin, M., Török, B. and Török, M. (2023). 'Structural features of small molecule antioxidants and strategic modifications to improve potential bioactivity', *Molecules*, 28(3), article number 1057. Available at: https://doi.org/10.3390/molecules28031057.

Chauhan, M., Saxena, A. and Saha, B. (2021). 'An insight in anti-malarial potential of indole scaffold: a review', *European Journal of Medicinal Chemistry*, 218, article number 113400. Available at: https://doi.org/10.1016/j.ejmech.2021.113400.

Cirillo, P.F., Caccavale, A. and DeLuna, A. (2021). 'Green Fischer indole synthesis using a steroidal ketone in a conductively heated sealed-vessel reactor for the advanced undergraduate laboratory', *Journal of Chemical Education*, 98(2), pp. 567–571. Available at: https://doi.org/10.1021/acs.jchemed.0c00991.

Dhiman, A., Sharma, R. and Singh, R.K. (2022). 'Target-based anticancer indole derivatives and insight into structure–activity relationship: a mechanistic review update (2018–2021)', *Acta Pharmaceutica Sinica B*, 12(7), pp. 3006–3027. Available at: https://doi.org/10.1016/j.apsb.2022.03.021.

El-Sayed, M., Mahmoud, K. and Hilgeroth, A. (2013). 'Glacial acetic acid as an efficient catalyst for simple synthesis of dindolylmethanes', *Current Chemistry Letters*, 3(1), pp. 7–14. Available at: https://doi.org/10.5267/j.ccl.2013.10.003.

Gong, P.-X., Jiang, Z., Meng, Y., Chen, H., Xiong, W., Zhang, W., Zhang, H., Chen, K., Miao, J. and Zhu, Y. (2025). 'Design, synthesis, and antifungal activity evaluation of novel hydrazide-containing *L*-perillaldehyde derivatives as potential fungicides', *Journal of Agricultural and Food Chemistry*, 73(36), pp. 22865 – 22876. Available at: https://doi.org/10.1021/acs.jafc.5c02794.

Gu, W., Wu, R., Qi, S., Gu, C., Si, F. and Chen, Z. (2012). 'Synthesis and antibacterial evaluation of new *N*-acylhydrazone derivatives from dehydroabietic acid', *Molecules*, 17(4), pp. 4634–4650. Available at: https://doi.org/10.3390/molecules17044634.

Guay, D.R. (2001). 'An update on the role of nitrofurans in the management of urinary tract infections', *Drugs*, 61(3), pp. 353–364. Available at: https://doi.org/10.2165/00003495-200161030-00004.

Halloran, M.W., Hudecek, C. and Burkart, M.D. (2023). 'Synthesis of acid hydrazides from carboxylic acids in continuous flow', *Organic Process Research & Development*, 27(9), pp. 1677–1683. Available at: https://doi.org/10.1021/acs.oprd.3c00216.

Hamzi, I., Barhoumi-Slimi, T.M. and Abidi, R. (2016). 'Synthesis, characterization, and conformational study of acylhydrazones of α,β-unsaturated aldehydes',

Heteroatom Chemistry, 27(3), pp. 139–148. Available at: https://doi.org/10.1002/hc.21310.

Hermanson, G.T. (2013). 'Chapter 11 - (Strept)avidin–biotin systems', in Hermanson, G.T. (3rd ed) *Bioconjugate techniques*. London: Academic Press, pp. 465–505.

Humphrey, G.R. and Kuethe, J.T. (2006). 'Practical methodologies for the synthesis of indoles', *Chemical Reviews*, 106(7), pp. 2875–2911. Available at: https://doi.org/10.1021/cr0505270.

Jasiewicz, B., Kozanecka-Okupnik, W., Przygodzki, M., Warżajtis, B., Rychlewska, U., Pospieszny, T. and Mrówczyńska, L. (2021). 'Synthesis, antioxidant and cytoprotective activity evaluation of C-3 substituted indole derivatives', *Scientific Reports*, 11, article number 15425. Available at: https://doi.org/10.1038/s41598-021-94904-z.

Kumar, P., Kadyan, K., Duhan, M., Sindhu, J., Singh, V. and Saharan, B.S. (2017). 'Design, synthesis, conformational and molecular docking study of some novel acyl hydrazone based molecular hybrids as antimalarial and antimicrobial agents', *Chemistry Central Journal*, 11(115), pp. 1-14. Available at: https://doi.org/10.1186/s13065-017-0344-7.

Lawrence, M.A.W., Lorraine, S.C., Wilson, K.-A. and Wilson, K. (2019). 'Review: voltammetric properties and applications of hydrazones and azo moieties',

Polyhedron, 173 (15), article number 114111. Available at: https://doi.org/10.1016/j.poly.2019.114111.

Le Goff, G. and Ouazzani, J. (2014). 'Natural hydrazine-containing compounds: bBiosynthesis, isolation, biological activities and synthesis', *Bioorganic & Medicinal Chemistry*, 22(23), pp. 6529–6544. Available at: https://doi.org/10.1016/j.bmc.2014.10.011.

Li, J., Ji, J., Xu, R. and Li, Z. (2019). 'Indole compounds with *N*-ethyl morpholine moieties as CB2 receptor agonists for anti-inflammatory management of pain: synthesis and biological evaluation', *Medicinal Chemistry Communications*, 10(11), pp. 1935–1947. Available at: https://doi.org/10.1039/c9md00173e.

Liang, N. and Kitts, D. (2014). 'Antioxidant property of coffee components: assessment of methods that define mechanisms of action', *Molecules*, 19(11), pp. 19180–19208. Available at: https://doi.org/10.3390/molecules191119180.

Lobo, V., Patil, A., Phatak, A. and Chandra, N. (2010). 'Free radicals, antioxidants and functional foods: impact on human health', *Pharmacognosy Reviews*, 4(8), pp. 118–126. Available at: https://doi.org/10.4103/0973-7847.70902.

Lopes, A., Miguez, E., Kümmerle, A., Rumjanek, V., Fraga, C. and Barreiro, E. (2013). 'Characterization of amide bond conformers for a novel heterocyclic template of *N*-acylhydrazone Derivatives', *Molecules*, 18(10), pp. 11683–11704. Available at: https://doi.org/10.3390/molecules181011683.

Łukasz Popiołek (2023). ‘The application of hydrazones and hydrazide-hydrazones in the synthesis of bioactive azetidin-2-one derivatives: a mini review’, *Biomedicine & Pharmacotherapy*, 163, article number 114853. Available at: https://doi.org/10.1016/j.biopha.2023.114853.

Luthra, T., Nayak, A.K., Bose, S., Chakrabarti, S., Gupta, A. and Sen, S. (2019). ‘Indole based antimalarial compounds targeting the melatonin Pathway: their design, synthesis and biological evaluation’, *European Journal of Medicinal Chemistry*, 168, pp. 11–27. Available at: https://doi.org/10.1016/j.ejmech.2019.02.019.

McKenzie, J.S., Donarski, J.A., Wilson, J.C. and Charlton, A.J. (2011). ‘Analysis of complex mixtures using high-resolution nuclear magnetic resonance spectroscopy and chemometrics’, *Progress in Nuclear Magnetic Resonance Spectroscopy*, 59(4), pp. 336–359. Available at: https://doi.org/10.1016/j.pnmrs.2011.04.003.

Mo, X., Rao, D.P., Kaur, K., Hassan, R., Abdel-Samea, A.S., Farhan, S.M., Bräse, S. and Hashem, H. (2024). ‘Indole derivatives: a versatile scaffold in modern drug discovery – an updated review on their multifaceted therapeutic applications (2020–2024)’, *Molecules*, 29(19), article number 44770. Available at: https://doi.org/10.3390/molecules29194770.

Moldoveanu, S.C. (2019). ‘Chapter 14 - Pyrolysis of various derivatives of carboxylic acids’, in Moldoveanu, S.C. (2nd ed) *Pyrolysis of organic molecules:*

applications to health and environmental issues. San Diego: Elsevier Science & Technology, pp. 635–696.

Munir, R., Javid, N., Zia-ur-Rehman, M., Zaheer, M., Huma, R., Roohi, A. and Athar, M.M. (2021). 'Synthesis of novel *N*-acylhydrazones and their C-N/N-N bond conformational characterization by NMR spectroscopy', *Molecules*, 26(16), article number 4908. Available at: https://doi.org/10.3390/molecules26164908.

Munteanu, I.G. and Apetrei, C. (2021). 'Analytical methods used in determining antioxidant activity: a review', *International Journal of Molecular Sciences*, 22(7), article number 3380. Available at: https://doi.org/10.3390/ijms22073380.

Neto, B.A.D., Beck, P.S., Sorto, J.E.P. and Eberlin, M.N. (2022). 'In melting points we trust: a review on the misguiding characterization of multicomponent reactions adducts and intermediates', *Molecules*, 27(21), article number 7552. Available at: https://doi.org/10.3390/molecules27217552.

Olugbami, J., Gbadegesin, M. and Odunola, O. (2014). In vitro evaluation of the antioxidant potential, phenolic and flavonoid contents of the stem bark ethanol extract of anogeissus leiocarpus', *African Journal of Medicine and Medical Sciences*, 43(1), pp. 101–109. Available at: https://pmc.ncbi.nlm.nih.gov/articles/PMC4679201/ (Accessed 6 Sep. 2025).

Ouellette, R.J. and Rawn, J.D. (2015). 'Chapter 19 - Aldehydes and ketones: nucleophilic addition reactions', in Ouellette, R.J. and Rawn, J.D. (1st ed) *Organic chemistry study guide: key concepts, problems, and solutions*. Amsterdam,

Netherlands: Elsevier, pp. 335–360. Available at: https://www.sciencedirect.com/science/article/pii/B9780128018897000194 [Accessed 8 Sep. 2025].

Özkay, Y., Tunalı, Y., Karaca, H. and Işıkdağ, İ. (2010). 'Antimicrobial activity and a SAR study of some novel benzimidazole derivatives bearing hydrazone moiety', *European Journal of Medicinal Chemistry*, 45(8), pp. 3293–3298. Available at: https://doi.org/10.1016/j.ejmech.2010.04.012.

Panaskar, A.N., Jain, A. and Mohanty, P.K. (2022). 'Synthesis and evaluation of anti-inflammatory activity of some chalcone hydrazide derivatives', *Journal of Pharmaceutical Research International*, 34(15B), pp. 18–26. Available at: https://doi.org/10.9734/jpri/2022/v34i15b35716.

PubChem (2020). *Indole*. Available at: https://pubchem.ncbi.nlm.nih.gov/compound/Indole (Accessed 4 Sep. 2025).

Rao, V.R. (2016). 'Chapter 7 - Antioxidant agents', in Penta, S. (1st ed) *Advances in structure and activity relationship of coumarin derivatives*. Amsterdam: Elsevier/Academic Press, pp. 137–150.

Reynolds, W.F. (2016). 'Chapter 29 - Natural product structure elucidation by NMR spectroscopy', in S.B. Mccreath, (2nd ed), *Pharmacognosy: fundamentals, applications and strategies*. Amsterdam: Academic Press, pp. 567–596. Available at: https://www.sciencedirect.com/science/article/pii/B9780128021040000299 (Accessed 9 Sep. 2025).

Schaller, C., Farmer, S., Kennepohl, D., Morsch, L., Soderberg, T. and Reutenauer, L. (2015). *13.10: Characteristics of ^{13}C NMR spectroscopy*. Available at: https://chem.libretexts.org/Bookshelves/Organic_Chemistry/Organic_Chemistry_(Morsch_et_al.)/13%3A_Structure_Determination_-_Nuclear_Magnetic_Resonance_Spectroscopy/13.10%3A_Characteristics_of_C_NMR_Spectroscopy (Accessed 9 Sep. 2025).

Shahidi, F. and Zhong, Y. (2015). 'Measurement of antioxidant activity', *Journal of Functional Foods*, 18(B), pp. 757–781. Available at: https://doi.org/10.1016/j.jff.2015.01.047.

Sharma, O.P. and Bhat, T.K. (2009). 'DPPH antioxidant assay revisited', *Food Chemistry*, 113(4), pp. 1202–1205. Available at: https://doi.org/10.1016/j.foodchem.2008.08.008.

Simijonović, D.M., Milenković, D.A., Avdović, E.H., Milanović, Ž.B., Antonijević, M.R., Amić, A.D., Dolićanin, Z. and Marković, Z.S. (2023). 'Coumarin *N*-acylhydrazone derivatives: green synthesis and antioxidant potential – experimental and theoretical study', *Antioxidants*, 12(10), pp. 1858–1875. Available at: https://doi.org/10.3390/antiox12101858.

Simoneau, C.A. and Ganem, B. (2008). 'A three-component Fischer indole synthesis', *Nature Protocols*, 3(8), pp. 1249–1252. Available at: https://doi.org/10.1038/nprot.2008.94.

Skeel, B.A., Boreen, M.A., Lohrey, T.D. and Arnold, J. (2020). 'Perturbation of $^{1}J_{C,F}$ coupling in carbon–fluorine bonds on coordination to Lewis acids: a structural, spectroscopic, and computational study', *Inorganic Chemistry*, 59(23), pp. 17259–17267. Available at: https://doi.org/10.1021/acs.inorgchem.0c02516.

Socea, L.I., Barbuceanu, S.-F., Pahontu, E.M., Dumitru, A.-C., Nitulescu, G.M., Sfetea, R.C. and Apostol, T.-V. (2022). 'Acylhydrazones and their biological activity: a review', *Molecules*, 27(24), pp. 8719–8719. Available at: https://doi.org/10.3390/molecules27248719.

Sulthana, R.M. and Quine, S.D. (2015). 'Synthesis, characterization, antibacterial evaluation and molecular docking studies of 2-azetidinone derivatives as novel DNA gyrase inhibitors', *International Letters of Chemistry, Physics and Astronomy*, 47, pp.94–108. Available at: https://doi.org/10.56431/p-l3nkhq.

Vlad, I.M., Nuță, D.C., Căproiu, M.T., Dumitrașcu, F. and Limban, C. (2024). 'Synthesis and characterization of new N-acyl hydrazone derivatives of carprofen as potential tuberculostatic agents', *Antibiotics*, 13(3), article number 212. Available at: https://doi.org/10.3390/antibiotics13030212.

Zhang, J., Liu, T., Chen, M., Liu, F., Liu, X., Zhang, J., Lin, J. and Jin, Y. (2018). 'Synthesis and biological evaluation of indole-2-carbohydrazide derivatives as anticancer agents with anti-angiogenic and antiproliferative activities', *ChemMedChem*, 13(12), pp. 1181–1192. Available at: http